FABRICATION OF A SEMICONDUCTOR INSULATOR SEMICONDUCTOR

PHOTOVOLTAIC CONVERTER

BY

NITIN V. KALAIYA

Thesis submitted in partial fulfillment for the degree

of Master of Science of the University of Nairobi

October 1990

DECLARATION

This thesis is my original work and has not been presented for a degree in any other University.
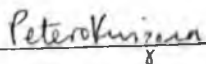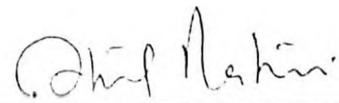
_____ 3/10/90

Nitin V. Kalaiya

University of Nairobi.

This thesis has been submitted for examination with the approval of my University Supervisors.

_____

Dr. Petero Kwizera

Department of Physics

University of Nairobi.

_____

Dr. Atul K. Raturi

Department of Physics

University of Nairobi.

ACKNOWLEDGMENTS

ABSTRACT

Semiconductor Insulator Semiconductor (SIS) Photovoltaic Converters have been fabricated successfully by the spray pyrolysis and the Vacuum deposition techniques . The two techniques and fabrication processes have been discussed. Preparation of Fluorine doped Tin Oxide films is also presented. SnO_2:F thin films with a sheet resistivity of $75\,\Omega/\square$ were deposited on $100\,\Omega$-cm P type (111) boron doped silicon wafer by spray pyrolysis and necessary contacts applied yielding an open circuit voltage of 110mV, short circuit current density of $45\mu A/cm^2$, fill factor of 0.25 and efficiency of 0.002% under $80mW/cm^2$ insolation.

Indium Tin Oxide thin films were deposited on similar silicon wafers using the vacuum coating unit and best values obtained for the cells were, open circuit voltage, 340mV, short circuit current density, $4.9mA/cm^2$, fill factor, 0.404 and cell efficiency 0.85%. Optical measurements of the films have been done and it has been found that the films are transparent and conducting.

The low efficiency can be attributed to high series resistance and possibly thick interfacial oxide layer.

CONTENTS

CHAPTER FOUR

SOLAR CELL FABRICATION BY VACUUM DEPOSITION

CHAPTER FIVE

CONCLUSION AND SUGGESTIONS FOR FUTURE WORK

LIST OF ILLUSTRATIONS

(vi)

CHAPTER ONE

INTRODUCTION

1.1 ENERGY SOURCES

In the seventies, critics favoured the utilization of nuclear power to other energy sources. 'little use has been made of (solar) cells in terrestrial operation, owing to the poor efficiency of the cells and their high costs' [1]. Taking a unit cell of an area of 10 square centimeters to collect 0.06% of all sunlight not reflected by clouds (about 6.10×10^{14} Kwh per year), the cells would require about 1% of all the land surface on the earth. This area is about 1 million square kilometers and if the cells operate at an efficiency of between 12 and 20%, the total number of cells required would be 10^{15}. Such projects look too remote and visionary.

With the World population at 4000 million, it is estimated that the annual energy requirement is 6.10×10^{14} Kwh. The Geothermal power taken over the entire land surface is less than 10^{14} Kwh per year. This source can only be used as a supplement. Wind and water power (including waves and tides), proved inadequate in the seventeenth and eighteenth centuries hence it is unlikely that they will stage a profound comeback in the twenty first century despite radically modern technology in this field. Hydropower has been the most successful by delivering about 10^{13} Kwh per year. In fact it delivers more energy in its operation than it consumes in its manufacture [2,3].

Critics declare that nuclear power is the prime mover in the future

and the only plausible alternative to our energy crisis [4]. The reasoning is that incidents of oil spills such as Canyon and the Amorco Cadiz (off the coast of Britanny in 1978) has served only to highlight the pollution menace [5]. The nuclear thermal yield is estimated at 2.10×10^{19} Kwh per year.

They have however been too naive in considering the overall cost of such plants and more important the disposal of atomic and nuclear wastes. Ironically, some of these wastes are converted into powerful energy sources viz weapons. The long term effects of radiation exposure on humans are far disheartening. Fossil fuels and Nuclear energy are already scarce, increasingly expensive and enviromentally hazardous. Their effects have respectively been highlighted recently by the Exxon's Alaskan disaster [6] and the Chernobyl disaster in the USSR [7].

1.2 SOLAR ENERGY

Rapid progress in solar energy research, development and application has taken place since the United Nations conference on new sources of energy was held in Rome in 1961. Solar research work has been supported by the International Solar Energy Society and its various international sections. In Japan, the sunshine project was established in 1974 under the Agency of Industrial, Science & Technology (AIST) of the Ministry of International Trade and Industry (MITI) to look into the utilization of solar energy for photovoltaic conversion and other uses. NASA's Jet Propulsion Laboratory in the U.S.A, has undertaken major projects in developing low cost solar cells.

The sun radiates in a continuous process of thermonuclear fission, approximately 8.33×10^{25} Kwh of energy per day of which the Earth receives about 4.41×10^{15} Kwh of energy [8]. Potential forms of energy dependent on the Sun's power include Oceans, the wind, hydropower, fossil fuels and biomass. Additionally the application of the first three may differ depending on the geographical and topographical characteristics of the terrain.

Solar light outside the atmosphere, called Air mass 0 (AM0) has a light intensity of 1.38 KwM^{-2}. The maximum light on ground at sea level is called Air mass 1 (AM1) with intensity of about 1 KwM^{-2} with a maximum of 1.1 KwM^{-2} on high mountains.

1.3 SOLAR CELLS

These devices convert light intensity into useful electrical power as explained in chapter two.

These cells has only been known for some thirty five years. Their advancement have been rather slow due to technical difficulties in manufacturing them.

Table 1 gives a brief chronological order in the development of the solar cell.

In 1954 a process was first developed for purifying silicon monocrystals. The basic silicon cell technology has been improved progressively since 1954. Current collector grids were used in 1960. Shortly afterwards, diffusion of the n layer by means of a P_2O_5 atmosphere, which is now a standard technique, was introduced.

3

Todate, the efficiency has remained between 5 to 20% [9,10].

Table 1: Development of the solar cell

Year	Comments
1930	Lange: first suggested solar cells for direct conversion of light into electrical energy.
1954	Pearson, Fuller, Chaplin: made first practical solar cell.
1954	First CdS thin film on glass.
1956	First terrestrial application for flash lights, navigation and communication stations.
1958	First solar cell on a satellite (vanguard 1).
1959	5% Polycrystalline cells.
1969	8% efficiency on CdS evaporated cells.
1974	Jordan: 5% achieved on lowcost spray deposited cells.
1977	12% ITO cell.
1978	12% SnO_2/Si cell.
1984	11% SnO_2:F-Si cell.
1987	15% p-n InP solar cell.
1989	17% ITO/InP cell.

Photovoltaic cells have already been identified as a major alternative to our energy crisis. Our local sources of energy are the Seven For scheme along the river Tana, Turkwell Gorge hydroelectric stations and the geothermal stations like the Ol Karia. With the unlimited supply of solar energy throughout the year, we can establish solar power stations. The most economical view is to manufacture the cells locally though this requires considerable investment in building furnaces for crystal growth, laboratories for doping the silicon and metalization etc. Large scale production can make the cells low cost and easily available mainly for rural electrification. We have an abundant supply of the chief raw material, silicon while other chemicals may be identified.

Several companies e.g. Total and Chloride Exide have successfully installed solar panels in rural areas of the country. However, the present cost of 30-40 thousand shillings per installation, is high and needs drastic cuts to be competitive. Some notable applications of solar cells throughout the world are cited in table 2.

Table 2: Some applications of solar cells.

Area	Application
California, U.S.A.	A 3 Kw ($85m^2$) photovoltaic system set up as a communication link.
Alaska	A solar powered 360W radio beacon.
Japan	A 6W robot rain gauge.
Indonesia	An unattended 130W navigational lighthouse.
Corsica, France	600W solar water pump.
Medina, Saudi Arabia	Solar powered navigation lights around the airport.
Japan	Use of solar cells in electronic calculators, computers and digital watches.
India	Solar water pumps.
Thailand	Remote village electrification project.

CHAPTER TWO

THEORETICAL ASPECTS

2.1 PHOTOVOLTAIC EFFECT

It is important to understand the photovoltaic effect applicable to semiconductors. The solar cells operate on this principle. The generation of electrical energy as a consequence of the absorption of ionizing radiation (photons) is known as the photovoltaic effect. The photons absorbed in a semiconductor releases their energies to electrons in the valence band, causing them to rise to the conduction band. In this process electron-hole pairs are created. The rate of pair generation at a distance x into the semiconductor is given by

$$G(\lambda,x) = \alpha(\lambda)N_o(\lambda)\exp[-\alpha(\lambda)x] \quad \dots\dots\dots\dots\dots\dots(1)$$

where $\alpha(\lambda)$ is the absorption coefficient for the wavelength λ and $N_o(\lambda)$ is the number of incident photons per unit area per second at that wavelength at the surface.

The absorptivity $\alpha(\lambda)$ is a quantitative measure of the ability of a material to absorb light of a given wavelength and is a measure in units of reciprocal distance. Silicon is an indirect bandgap material i.e. the maximum of the valence band and the minimum of the conduction band occur at different values of K. For a transition to take place, the electron must lose momentum by releasing a phonon. Trap levels are set up within the forbidden region via which electron-hole recombination takes place. Absorption takes place when photon energy equals bandgap energy in case of silicon. The

7

incident light of shorter wavelength (ultra-violet) is absorbed
close to the surface and the photons due to infrared radiation, deep
in the bulk or not at all. $\alpha(\lambda)$ decreases with λ.

Initially a built in field separates the charges (electron/holes).
The separation of charges produces a forward voltage across the
barrier. Forward because electric field of the photo-exited carriers
is opposite to the built in field of the junction. In practice p-n
junctions of silicon can be used to convert solar energy to
electrical energy. A p-n junction must be created to move carriers
to the edge of the semiconductor (Fig.1).
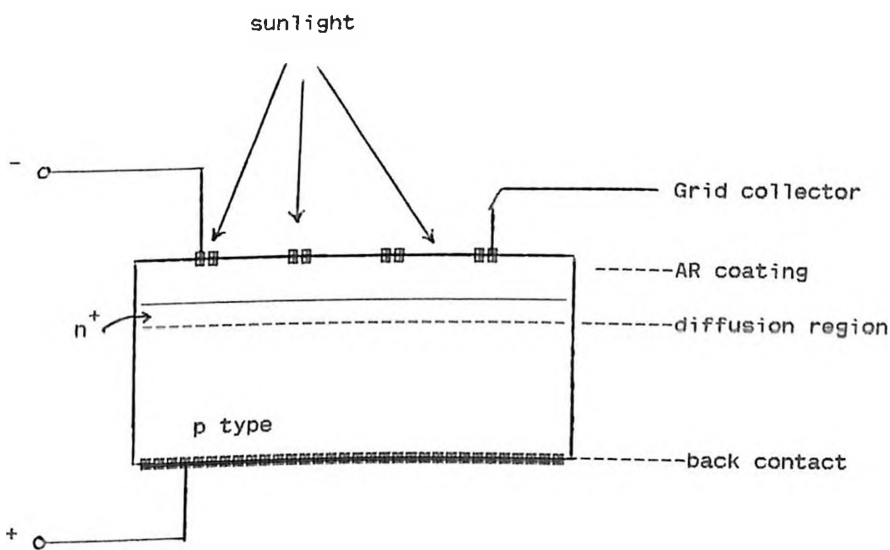
Fig.1 p-n Junction Solar Cell with Diffused n^+ Region into
p Base Semiconductor.

2.2 SILICON WAFERS

Silicon is the most successful and widely used photovoltaic energy
converter material. Silicon is mainly used because of its relative
abundance, reliability, stability, the backlog of information and

8

experience in silicon cell manufacturing technology. The thin film technology holds the greatest potential for material conservation, simplified growth techniques and the process scaling feasibility necessary for mass production [11].

The high costs of silicon used in solar cells is due to the purification of the silicon from metallurgical to semiconductor grade, using conversion of Si into $SiHCl_3$, purification of $SiHCl_3$ and reconversion into Si. The steps are very energy intensive as well as expensive. The silicon wafers can be manufactured in the following sequence [12];

(a) Conversion of metallurgical silicon to trichlorosilane by distillation and other means.

(b) the preparation of polycrystalline silicon by the hydrogen reduction of trichlorosilane.

(c) growth of silicon single crystal of controlled purity from the polycrystalline material by melt growth techniques.

(d) the preparation of silicon wafers of at least 0.2 mm thickness by cutting the single crystal ingot, followed by polishing.

Silicon ingots are grown by unidirectional freezing using the Czochralski crystal growth method. Several other high speed, potentially lowcost Si sheet growth techniques are available which includes the Stepanov process (non wetted die), dip coating of a ceramic substrate, hot rolling, chemical vapour deposition (cvd) on glass or ceramic substrate, photo-cvd and glow discharge decomposition of silane [13].

9

2.3 SOLAR CELL OPERATION

A basic silicon p-n junction is created by an appropriately boron doped (p type) single crystal substrate being diffused by phosphorus to create a shallow (0.2-0.5μm) n type layer (Fig.1). The n layer (front surface) is contacted by a metal grid designed to cover only a small percentage of the surface, while the p layer is contacted at the back by a metal covering the complete surface. An antireflection coating is used on the front to minimize reflections from the silicon surface between the grid fingers, and a cover glass is employed to protect the device in the working environment.
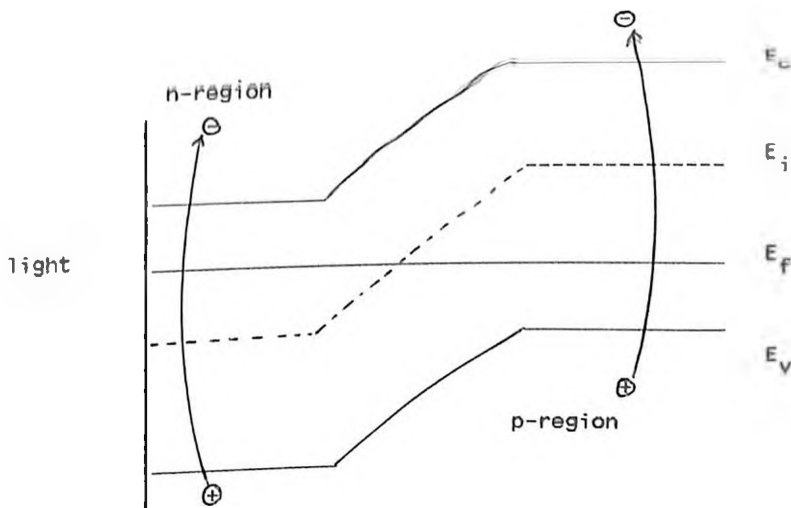
Fig.2 One Dimensional Energy Band Diagram Through Non Metallized Region of Cell.

When light is incident on the top surface of the cell, excess minority carriers cross the junction (Fig.2). If no external connections are made, a voltage will build up across the depletion region as charge separation occurs, forward biasing the p-n junction. At steady state the voltage produces diode injection

10

current which equals the photo current and an open circuit voltage (V_{oc}) condition is established (Fig.3).
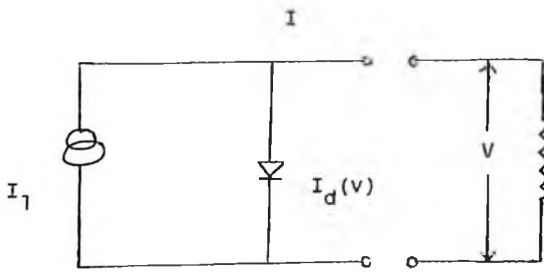
Fig.3 Open Circuit Voltage with External Load.

With an external load connected, the voltage across the diode will be reduced from the open circuit value, hence the diode injection current will be reduced and the external current will be the difference between the photocurrent I_1 and diode current (dark current) $I_d(v)$. The depletion region acts as space charge recombination region in a forward biased diode, giving rise to current flow. Thus

$$I_o(v) = I_1 - I_d(v) \quad \dots\dots\dots\dots\dots\dots(2)$$

The basic semiconductor device equations for a one dimensional case are [14];

    (a) Current transport equations

$$J_n = q\mu_n nE + qD_n dn/dx \quad \dots\dots\dots\dots\dots(3)$$

$$J_p = q\mu_p pE - qD_p dp/dx \quad \dots\dots\dots\dots\dots(4)$$

    (b) continuity equations

$$\partial n/\partial t = G - U + 1/q \, dJ_n/dx \quad \dots\dots\dots\dots(5)$$

$$\partial p/\partial t = G - U - 1/q \, dJ_p/dx \quad \dots\dots\dots\dots(6)$$

    (c) Poisson's equation

$$\partial E/\partial n = q/E \, (N(x) - p - n) \quad \dots\dots\dots\dots(7)$$

where J_n and J_p are electron and hole current densities respectively, E is the electrostatic field, μ is the mobility, D is the diffusion coefficient, q is the electronic charge and $N(x)$ is the impurity density distribution. G, the generation rate due to light, is the integral over all wavelengths λ of the right hand side of equation (1). The term U is the net thermal recombination-generation rate, modeled by Shockly-Read-Hall in terms of a trapping level located in the bandgap

$$U = \frac{pn - n_i^2}{\tau_{po}(n + n1) + \tau_{no}(p + P1)} \quad \dots\dots\dots\dots(8)$$

here n_i is the intrinsic carrier density, τ_{po} and τ_{no} are minority hole and electron lifetimes respectively, n1 and p1 are the electron and hole densities which would exist if the fermi-level were located at the trapping level.

Considering diffusion only and ignoring G, the dark current density of the diode is given by

$$J_d(v) = J_o[\exp(qV_j/KT) - 1] \quad \dots\dots\dots\dots\dots(9)$$

I_d and I_o in eqn (2) are simply J_d and J_o (reverse saturation current density) multiplied by the total area of junction. For a non ideal case the dark current can be represented by

$$I_d(v) = I_o[\exp(qV/nKT) - 1] \quad \dots\dots\dots\dots\dots(10)$$

where n is the ideality factor with values between 1(ideal) and 2, q, the electronic charge, V, applied voltage, K, Boltzman constant and T, the diode temperature.

12

2.4 CELL CHARACTERIZATION

If the back and front contacts of a cell are connected to one another, a current flows from the front to the back contact without any voltage. This is the maximum current across the diode and is termed as the SHORT CIRCUIT CURRENT. The total diode current under illumination is given by

$$I = I_1 + I_0(1 - e^{qV/KT}) \qquad \ldots\ldots\ldots\ldots\ldots\ldots(11)$$

where I_0 is the saturation current, I_1 is the light generated current and the second term is the reverse diode current. For uniform absorption,

$$I_1 = qG_1(L_n + L_p)A \qquad \ldots\ldots\ldots\ldots\ldots\ldots\ldots(12)$$

where G_1 is the generation rate.

In an open circuited cell, no current flows but the voltage generated is maximum. Setting $I=0$ in eqn(11), the OPEN CIRCUIT VOLTAGE is [15,16]

$$V_{oc} = (KT/q)\ln(1 + I_1/I_0) \qquad \ldots\ldots\ldots\ldots\ldots\ldots(13)$$

the open circuited voltage source can supply a current if an external load is connected across it. The power delivered to the load is thus

$$P = IV = I_1V - I_0V(e^{(qV/KT)} - 1) \qquad \ldots\ldots\ldots\ldots(14)$$

The voltage corresponding to maximum power delivery V_{mp} is obtained by taking $\partial p/\partial v = 0$ in eqn(14). Hence

$$(1 + qV_{mp}/KT)e^{(qV/KT)} = 1 + I_1/I_0 \qquad \ldots\ldots\ldots\ldots(15)$$

13

current at maximum power is denoted by I_{mp}. The SOLAR CELL EFFICIENCY is

$$n = (I_{mp}V_{mp}/P_{in}) \times 100\% \qquad \dots\dots\dots\dots\dots\dots(16)$$

where P_{in} is the input light power.

I_1 and V_{oc} are the maximum current and voltage respectively achieved in a solar cell. FILL FACTOR is defined as the ratio,

$$V_{mp}I_{mp}/V_{oc}I_{sc}$$

This is useful as a measure of the realizable power from the I-V curve. Typical values for a commercial cell lie in the range 0.7 to 0.8. I_{sc}, is the short circuit current.

For an ideal solar cell the series resistance is zero and the shunt resistance is infinity. Commercial cells have series resistance in the range of 1 to 5Ω. Series resistance (Rs) is due to the resistivity of the bulk materials, the resistance of the depletion region and resistance of the contacts. Shunt resistance (Rsh) results from junction defects which determine leakage current across junction (Fig.4).
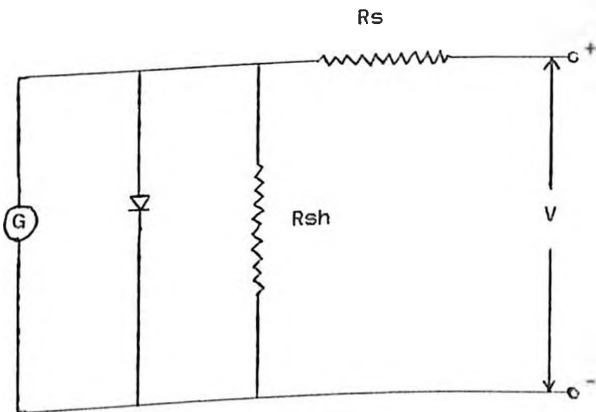
Fig.4 Equivalent circuit of a solar cell

14

The series resistance of the cell is obtained by illuminating the cell at two different intensities and plotting their I-V characteristics [17].
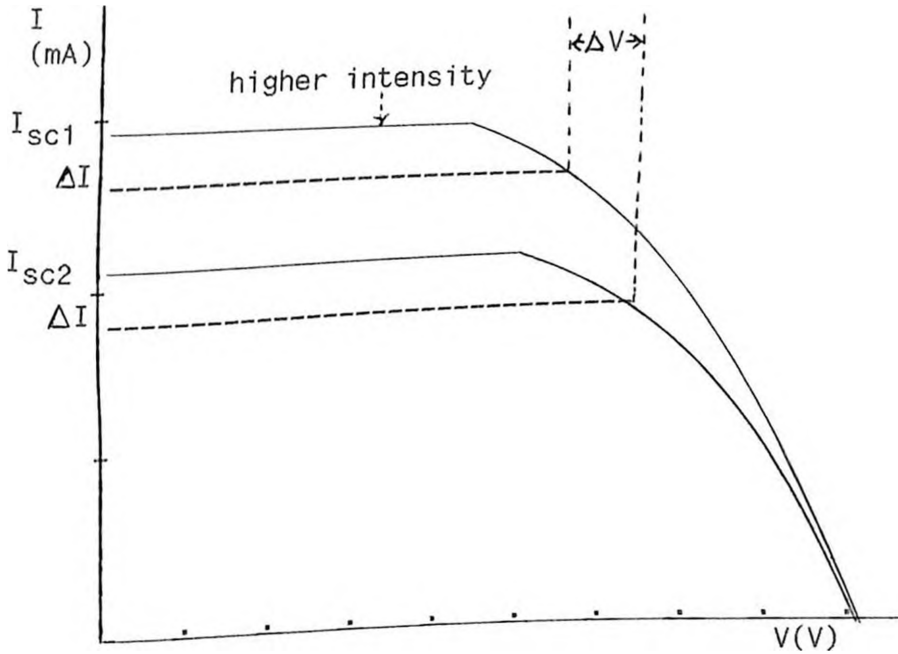
Fig.5 I-V characteristics at two different intensities

Series resistance Rs from above is

$$Rs = V/(I_{sc1} - I_{sc2}) \quad \dots\dots\dots\dots\dots(17)$$

The series resistance can also be obtained from the dark I-V characteristics of the cell. The equation for such a case is

$$I = I_0[exp(e/nKT)(V - IRs) - 1] \quad \dots\dots\dots\dots(18)$$

where I_0 is the saturation current and Rs is the series resistance The carrier lifetime is determined by

$$dV_{oc}/dt = -nKT/qt \quad \dots\dots\dots\dots\dots\dots\dots(19)$$

15

where K is the Boltzman constant, q is the charge of an electron, n is the ideality factor, t the base time and T, the temperature.

2.5 MIS AND THE SIS SOLAR CELLS.

2.5.1 INTRODUCTION

The SIS (semiconductor insulator semiconductor) diode or heterojunction is a device on which one side is a wide band gap semiconductor and the other a much narrower band gap material, such as silicon. The wide band gap semiconductor serves to block band to band majority carrier current and thus, in principle, gives a better device performance than with an MIS (metal-insulator) solar cell.

To enhance the photovoltaic barrier or junction, an ultra thin metal or a relatively thick transparent (wide band gap) conducting semiconductor, such as Indium Tin Oxide (ITO) or Tin Oxide, is deposited on the top surface. An oxide layer (10-30 Å) is grown between the top deposited contact and the base semiconductor. This type of cells are referred to as the MIS or SIS (Fig.6).
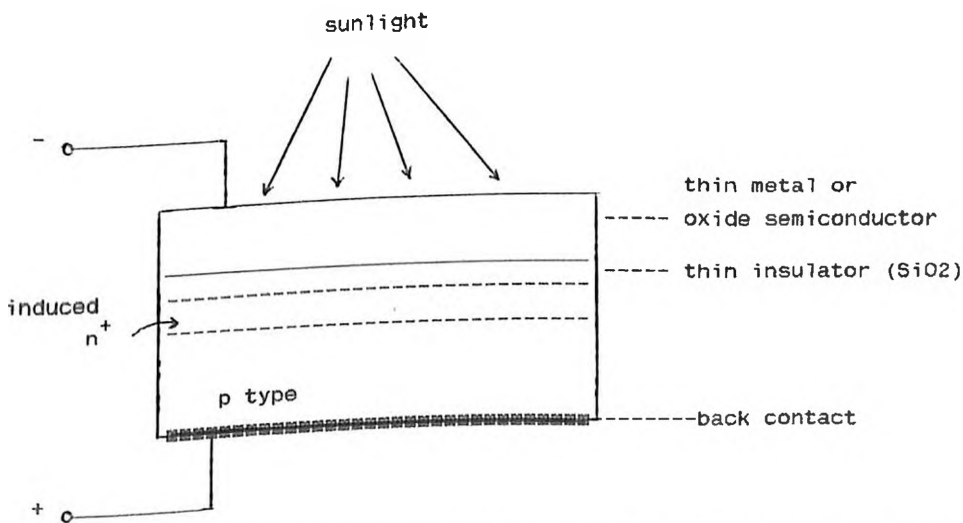
Fig.6 MIS or SIS Solar Cell with Thin Interfacial Layer.

16

The metals which have been used on Metal-SiO_2-Si configuration includes low workfunction (< 3.6eV) Al, Cr, Ta, Ti on p type silicon and high workfunction (> 3.6eV) metals, Au, Ag, Cu, Ni, Pt on n type silicon. GaAs has also been used in place of silicon in an MIS configuration[18]. The MIS cell may be considered to some extent as a limiting case of the SIS cell with the former having top metal layer and the latter a transparent conducting semiconductor with a band gap of 3.6 eV. The two belong to a family of solar cells known as the conductor-insulator-semiconductor (CIS).

2.5.2 THEORETICAL BACKGROUND

Cells with a thin layer of insulator between the metal and semiconductor, dramatically control the characteristics of the junction. If the insulator is made sufficiently thin (< 60Å), then quantum mechanical tunneling currents could flow through the insulator and couple to the induced p-n junction. Also in case of such a film, a non equilibrium mode of operation is possible in which the induced p-n junction functions normally, as in the diffusion formed case, over a certain range of bias or potential difference. The current transport, which takes place through diffusion in the thin layer merely provides an ohmic contact.

Oxides applied to silicon can also achieve good photovoltaic efficiency. The metal is replaced by a transparent (wide band gap) conducting semiconductor. These oxides are generally SnO_2, In_2O_3 or a mixture of both. The MIS diode requires a thin (~50Å) metal film in order to permit sufficient transmission of light, whereas the SIS has several thousand Å of conducting oxide layer because it

17

is largely a transparent medium. The conducting medium must be degenerately doped. The SIS structure greatly reduces or eliminates the requirement of a collection grid. Anti-Reflective top coatings are preferred for this configuration. The refractive index n, of silicon lies between 3 and 6 depending on the doping levels. The ideal n_z for the AR coating is,

$$n=\sqrt{n_1 n_2} \qquad \ldots\ldots\ldots\ldots\ldots\ldots\ldots(20)$$

where n1 being equal to one for air, gives n to be about 2. The refractive index of the materials used should be in this range, providing an advantage in that they can be used as partial AR coatings [19].

2.5.3 SIS JUNCTION

Structurally, the two semiconductors are separated by an interfacial region, but the exact nature of the transitions on either side of the interface is not known. As a first approximation, a sharp interfacial layer model is considered even though the semiconductor-to-insulator transitions are more likely to be graded. The behavior of the SIS diode is not particularly sensitive to these transitions. The current transport through the insulator (10-30Å) takes place through tunneling of minority carriers which in effect provides an 'ohmic contact'.

The system (Fig.7) is an ITO-SiO_2-(p type)Si. E_{gos}, E_{gi} and E_{gs} denote the bandgap of ITO, SiO_2 and Si respectively. Φ_b is the barrier height which governs the V_{oc} of the device. Φ_{osi} is the oxide semiconductor-to-insulator barrier height and is related to the work function of ITO .

18

insulator

$\bar{\Phi}_{si}$=3.2 eV
semiconductor

surface states

$\bar{\Phi}_{osi}$=3.2eV

E_{gi}

metal
ohmic

E_{gs}

E_f

contact

Φ_b

E_{gos}=3.6eV

neutral
region

depletion layer
inversion layer

semiconductor

d
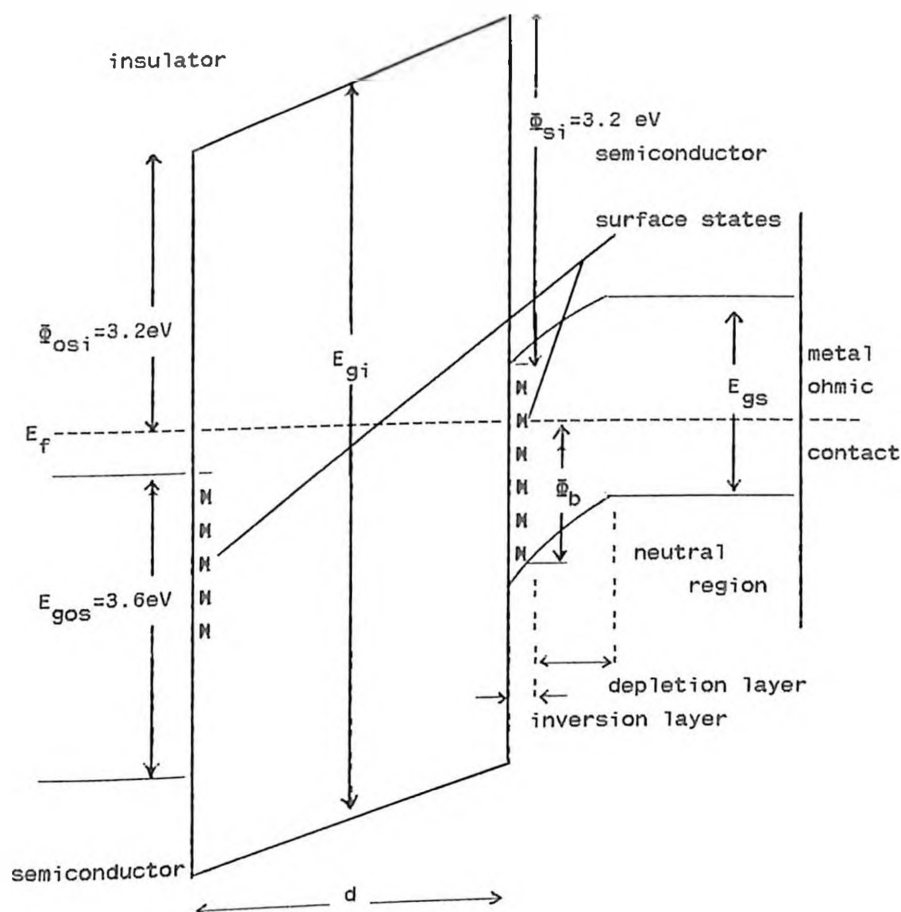
Fig 7 *Schematic Diagram (Energy Band) of the SIS Tunnel
Diode Under Equilibrium Conditions.*

The 'thickness' of the interfacial layer is a dominant parameter in
that as thickness (d) increases, the output of the cell falls
dramatically. The wavefunction of the charge carrier is of the same
order of magnitude in extent as the interface. Thus part of the
wavefunction can penetrate the interface and appear on the
otherside, which constitute a current flow (Fig 7). The surface of
the p type silicon is inverted by virtue of the ITO and Si work
functions where ITO is regarded as a low work function material. A
high work function material ($\bar{\Phi}_{osi}$ > 3.6 eV) would yield a surface

19
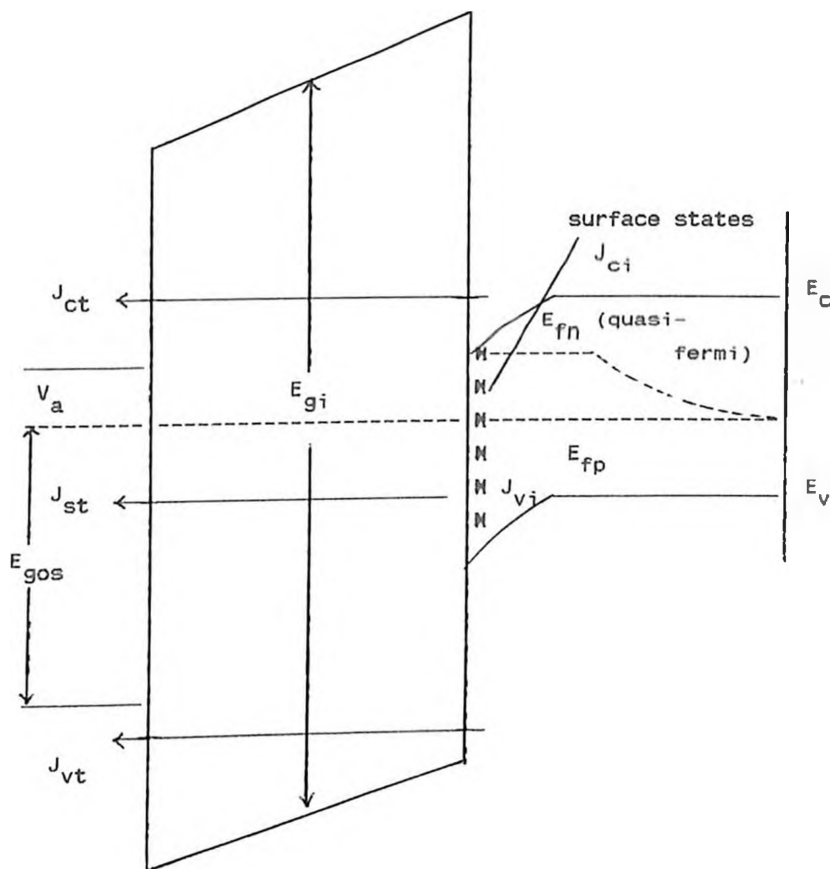
Fig.8 Schematic Energy-Band Diagram of the Minority- Carrier ITO -SiO_2-(p-type)Si Tunnel Diode System Under Zero Illumination.

which is accumulated rather than inverted.

In Fig.8, the device is biased positively by a voltage V_a with respect to the top ITO layer . J_{st} is a flow of current to the ITO supplied by J_{ci} and J_{vt}. J_{ct} and J_{vi} are the current flows from the conduction and valence bands of the Si to the ITO layer. The electron and hole fermi levels in the semiconductor are also shown.

The inverted p silicon surface provides a supply of minority carriers (electrons) which can tunnel into the ITO (J_{ct}). Majority carriers are blocked from tunneling by the ITO bandgap. Tunneling

20

can also occur via defect states at the two interfaces. J_{st} can be regarded as the dominant tunnel transition via defects in ITO-Si. J_{ci} and J_{vi} are the effective coupling current flows due to the interchange of charge between the conduction and valence bands of the silicon by recombination-generation process. The initial currents are low and the semiconductor is in 'thermal equilibrium'. The device operates as a capacitor, hence voltage drop can be determined by a solution of the Poisson's equation.

As thickness is decreased (<60 Å), the system departs from 'thermal equilibrium'. At about 30 Å thickness, the diode current is semiconductor limited (by the generation-recombination process in the bulk) and the tunnel current merely acts as an ohmic contact. The type of diode depends on the order in which the semiconductor surfaces at the semiconductor-insulator interfaces are either accumulated, depleted, or in strong inversion and the respective band gaps of the semiconductors. The diodes can hence be accordingly classified as majority carrier, surface states, or minority carrier devices depending on whether the dominant tunnel current flowing near zero bias is between the majority-carrier bands, surface states, or the minority-carrier bands. The state of the semiconductor surface is determined largely by the work functions of the semiconductors. The wide band gap of the ITO (~3.6 eV), inverts the surface of the p type silicon and blocks the majority carriers which may take part in a band to band tunneling hence this structure is a minority-carrier nonequilibrium SIS tunnel diode. By inverting the p type silicon surface, an electrostatic p-n junction is created. Any barrier (Φ_{osi}) less than about 3.6 eV is

21

sufficient to do this.

Figure (8) shows the SIS diode under forward bias V_a. In this mode of operation the minority-carrier quasi fermi levels in the semiconductors can be pinned effectively to their respective minority-carrier band edge over a limited bias range. This means that the carrier concentration at the surface is essentially fixed.
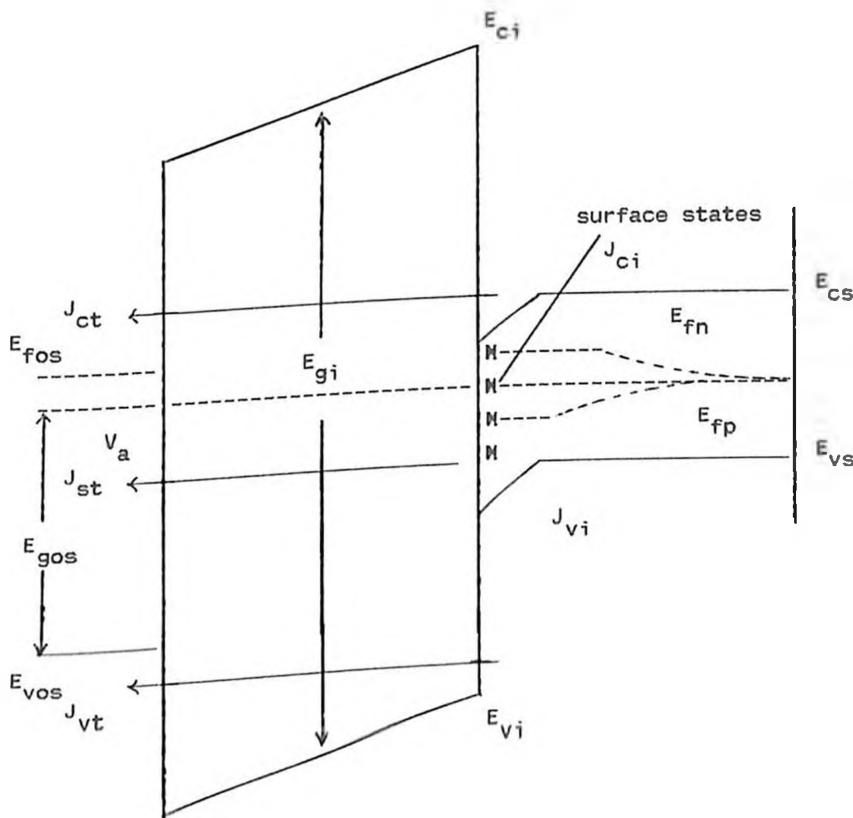
Fig.9 Energy Band Diagram of the ITO-SiO$_2$-(p-type)Si Tunnel Diode
System Near the Maximum Power Conditions Under Illumination.

The tunnel limited operation is approached with forward biasing the junction whereby the tunnel current is no longer an 'ohmic contact'. At the start, the electron-fermi level becomes unpinned with respect to the conduction band edge. Prior to this bias point, the SIS

22

diode operates as a pseudo p-n junction and, in absence of defects, would be an ideal shockly diode.

Figure (9) shows a band diagram with the diode operating in a photovoltaic mode near maximum power point. The electron and the hole quasi-fermi levels reflect the light-induced generation of carriers [20]. The band gap of the transparent medium helps in blocking the majority carriers from the valence band of the base semiconductor.

SOLAR CELL FABRICATION BY SPRAY PYROLYSIS

3.1 INTRODUCTION

The spray pyrolysis technique is a versatile method which has been used successfully in glassworks, metal coatings, semiconductor device manufacturing etc. It is a major process employed in the chemical vapor deposition (CVD) of metal and alloy thin films which is normally done by the thermal decomposition or pyrolysis of organometallic compounds, hydrides and metal hydrides generally at low temperatures.

The importance of spray pyrolysis lies primarily in its versatility for depositing a very large variety of elements and compounds at a relatively low temperature, in the form of both vitreous and crystalline layers having a high degree of perfection and purity. The method is basically a material synthesis in which the constituents of the liquid phase react to form a solid film at some surface [21].

One of the challenges to preparing high quality films by spray pyrolysis is to minimize the high porosity and gross texturing that is associated with volume shrinkage and the evolution of gaseous by products.

3.2 THIN FILMS

Thin film techniques are recognized to be among the most promising ways of producing low cost solar cells. The advantages of thin film cells are that very little of the expensive semiconductor material is needed, low cost substrate can be used and simplified growth techniques and process scaling feasibility is required for mass production. Their disadvantage lies mainly in the low efficiencies obtained, due partly to the grain boundary effects and partly to the poor quality of the semiconducting material that often results from growth upon foreign substrates. A great deal of research is being undertaken in this field [22]. Spray pyrolysis is a thin film technique.

A wide range of thin film solar cells already exists in the market. This includes the heterojunction, p-i-n junction, schottky barrier the metal-insulator-semiconductor (MIS) and the metal oxide semiconductor (MOS) cells [23].

3.3 EXPERIMENTAL SETUP

The principle of obtaining a fine spray is by passing a liquid and gas through a fine capillary outlet. The sprayer made of glass, has two inlets, one for the liquid and one for the gas and a single outlet. Nitrogen or Argon gas can be used though the former is preferred due to the low cost. Glass slides (1.0 x 3.5 cm) are thoroughly cleaned by using a detergent and then acetone. These are then placed on a hot plate whose temperature is controlled by a

variac. The temperature can be obtained by means of a thermocouple and a multimeter [24]. From a suitable height, the solution is sprayed on the glass slide for a few seconds and then the spraying is stopped to allow the temperature of the hot plate to rise back to the optimum value ($400^{\circ}C$). The process is repeated a few times until a thin film is formed on the glass substrate (Fig 10). To obtain a uniform film, the sprayer is moved over the slides slowly while spraying.
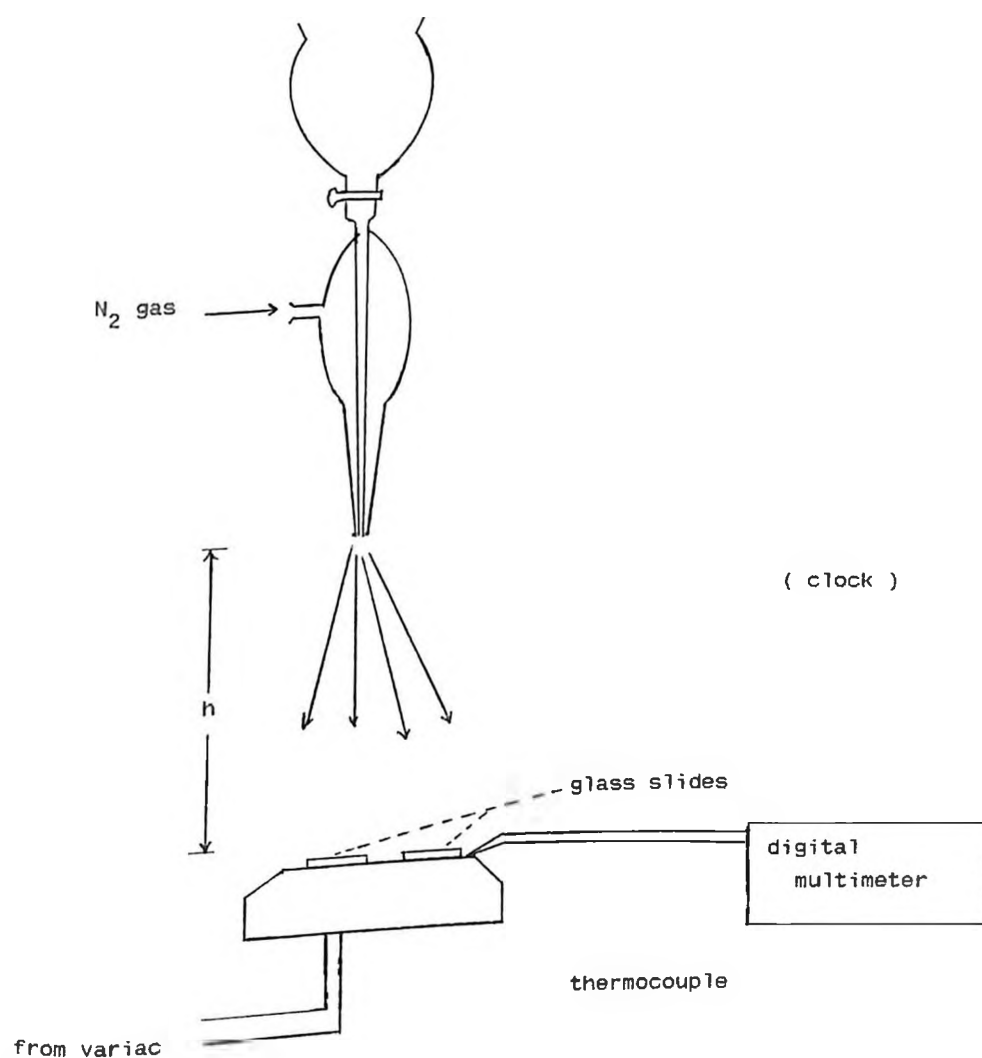
Fig 10 *Experimental Set Up of the Spray Pyrolysis System.*

3.4 FILM PREPARATION

An alcoholic solution of stannic chloride is prepared at various
concentrations using suitable ratios of $nSnCl_4:xC_3H_7OH:yH_2O$ by
weight percentage (appendix A1). The required mass of stannic
chloride is dissolved in propanol and some distilled water is added.
This mixture is then sprayed on the glass substrate at about $400^{\circ}C$.
The spraying is done for ten seconds and repeated at intervals of 2
minutes when optimum temperature is attained. Films of tin oxide
are formed on the glass slides.

Fluorine doped tin oxide films are also deposited on fresh slides.
This solution is prepared in the ratio $qSnCl_4:xC_3H_7OH:yH_2O:pNH_4F:$
$zHCl$ by weight percentage (appendix A2).

The transmission of light through the films is measured by the
Perkins Lambda 9 spectrophotometer. The conductivity of the tin
oxide layer is measured by painting two strips of conductive paint
at the edges of the film and placing probes connected to a
multimeter.

3.4.1 Cell Fabrication

A 100 Ω-cm P type (111) boron doped silicon wafer is cleaned in
acetone and then dipped into a buffered HF solution to remove the
native oxide. Ammonium fluoride is used to buffer the solution so
that fluorine ions are not depleted. After fifteen seconds the
wafer is thoroughly rinsed in distilled water and an oxide layer is
grown by placing the wafer in concentrated nitric acid at 60 $^{\circ}C$ for

27

about twenty seconds. The wafer is again cleaned by distilled water. This process is similar to one used by S. P. Singh et al. [25].

Aluminium back contact is applied to the un-polished side of the wafer by using the vacuum coating unit. The substrate is then placed on a heater at 350 ^{o}C and tin oxide layer is grown by spray pyrolysis. Silver grid is applied to the cell by placing a grid mask on top of the polished side of the substrate (on which a tin oxide layer has been grown) and depositing silver by using the vacuum coating unit.

3.5 RESULTS

Table 3 gives the effects of temperature on the films. Preliminary results gave the best spray height of about 40cm, temperature of 400°C and gas pressure of 14-18 Pa.

Spray heights above 50 cm consummed too much of the solution and too low height produced thick non-uniform films. The experiment is performed in a fume chamber to reduce the effects of gaseous by-products on the user. Tables 4 and 5 gives various concentrations of undoped and doped SnO_2 films and their respective sheet resistivities.

Table 3: Effects of deposition Temperatures on SnO_2 Films.

Temperature (^{O}C)	Film Description
200	Non uniform clustered film
300	Smaller droplets on film. High porosity
350	'Orange Peel' effect, tiny porous holes
400	Uniform and clear film
480	Slightly cracked film

Table 4: Concentrations of Solutions and sheet resistivities of SnO_2 films.

Sample number	% Concentration			Sheet resistivity $\Omega/\square$
	$SnCl_4$	C_3H_7OH	H_2O	
01	13	32	55	1.5×10^4
02	20	40	40	1.0×10^4
03	30	35	35	4.7×10^3
04	35	33	32	3.5×10^3
05	29	30	41	1.1×10^3
06	25	44	31	8.5×10^2

Table 5: Fluorine doped SnO_2 films.

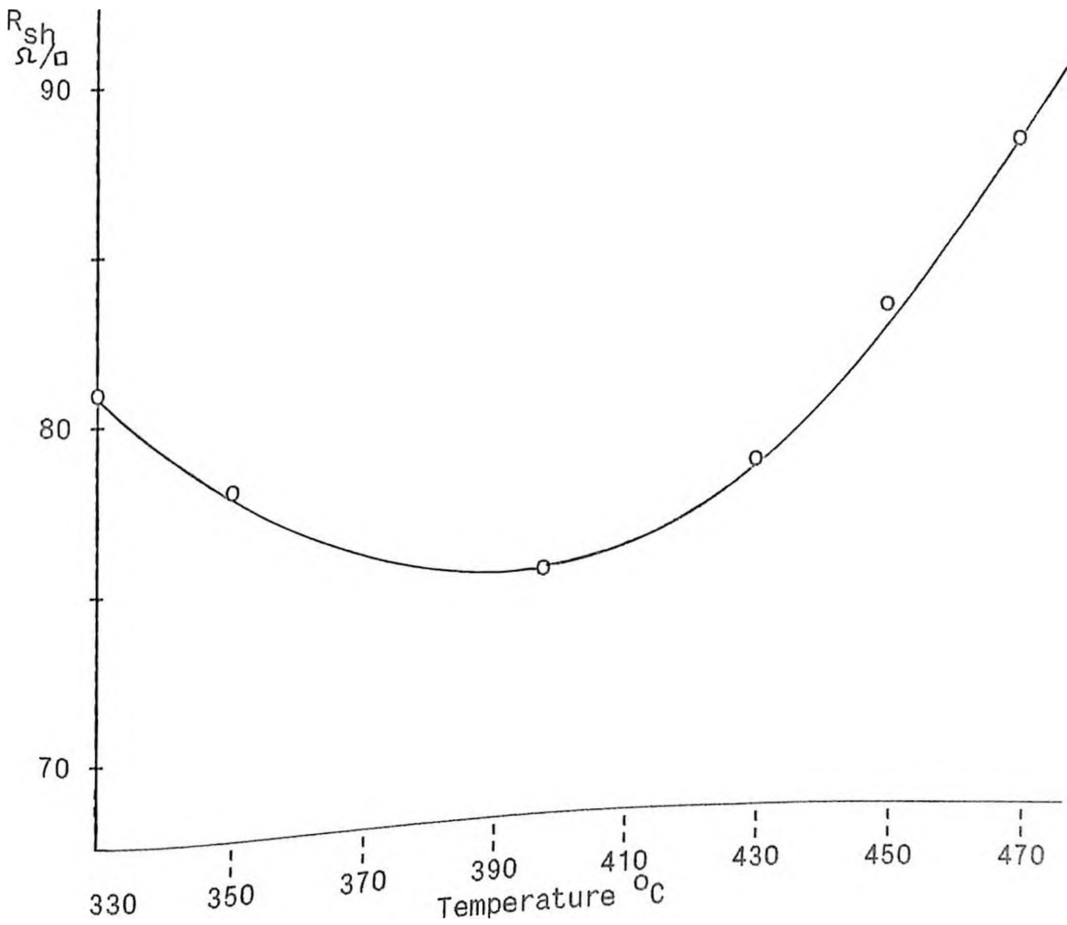| Sample number	% Concentration					Sheet Resistivity
	$SnCl_4$	C_3H_7OH	H_2O	NH_4F	HCl	
10	13	32	52	3	0	1.5×10^3
11	15	34	49	1	1	1.3×10^3
12	36	20	40	2.5	1.5	3.2×10^3
13	29	30	37.5	2	1.5	2.0×10^2
14	28	39.5	29	1.5	2	7.5×10

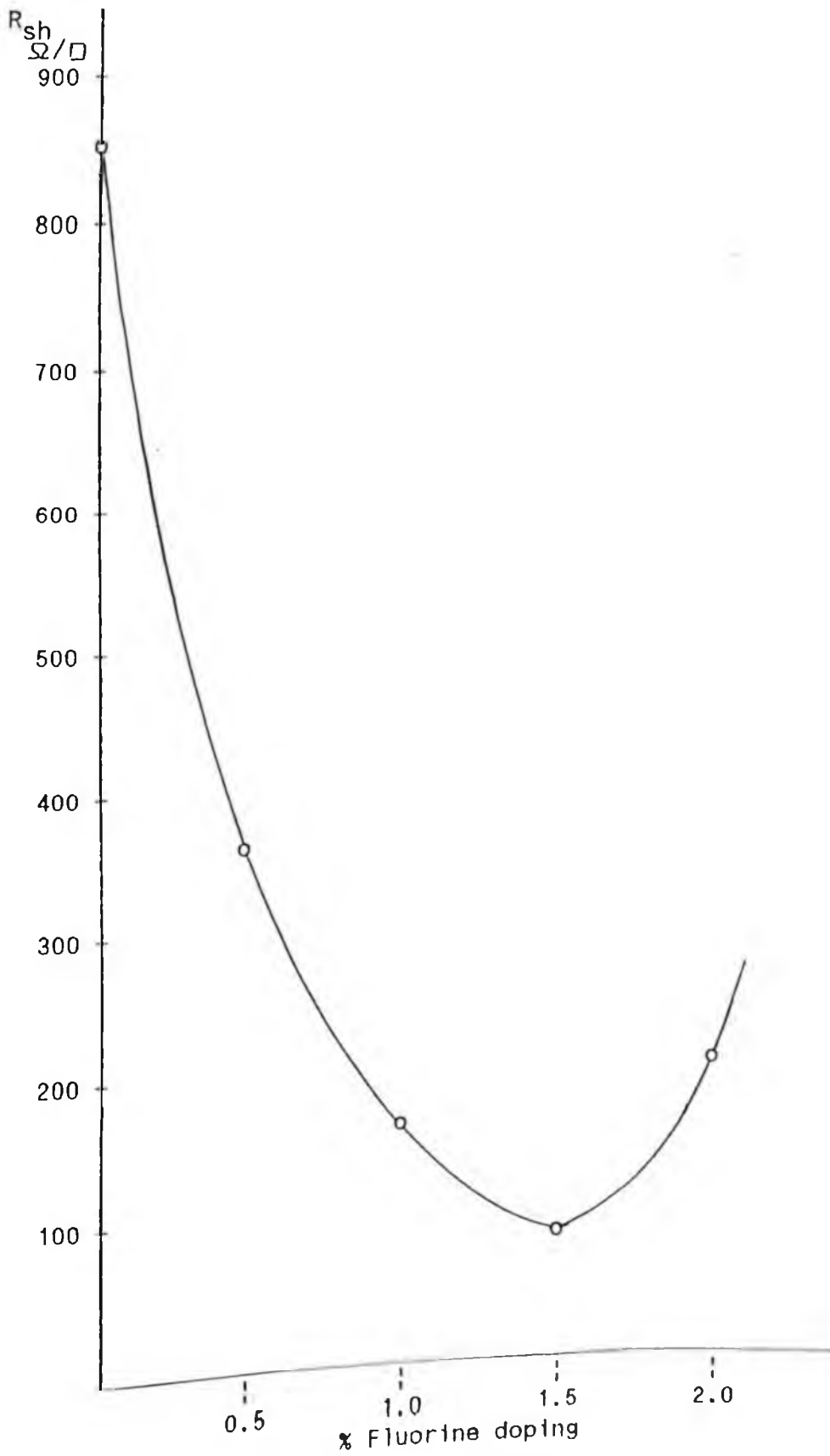Fig.11 Graph to show variation of sheet resistance with depositon temperature.

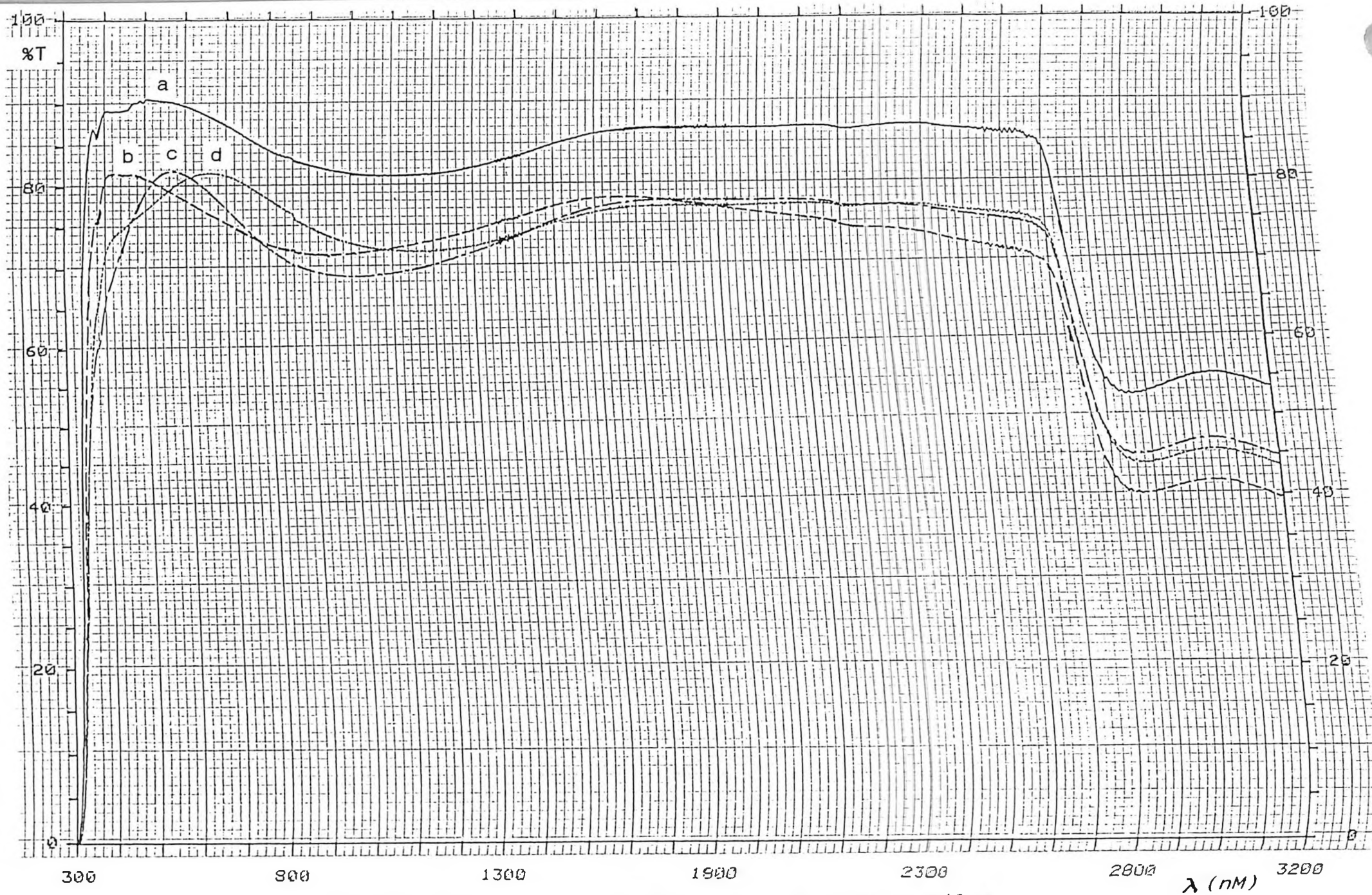Fig. 12 Variation of sheet resistivity with % Fluorine doping at 400 °C

Fig.13: Transmission through: (a & b) SnO_2:F Films,
(c & d) SnO_2 Films at room temperature.

32
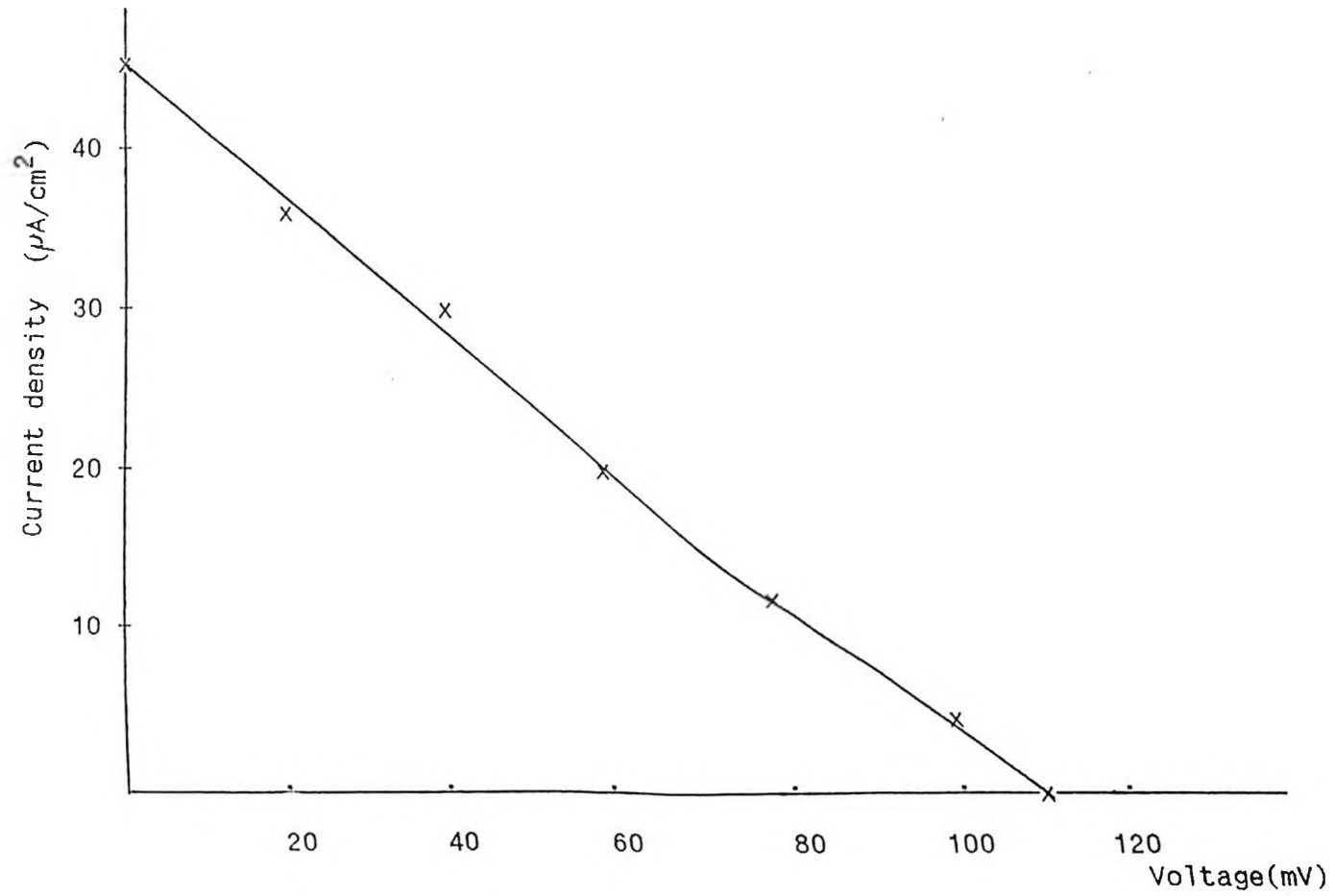
Fig.14: Power curve of an SnO_2:F-p Silicon solar cell.

33

3.6 DISCUSSION

The stannic oxide films on visual inspection show a bluish hue. Very finely sprayed films may show indigo-purple tint as well. The stannous oxide films are greenish yellow. The optimum solution for undoped SnO_2 films contain 25 wt.% $SnCl_4.5H_2O$, 40 wt.% C_3H_7OH and 35 wt.% H_2O deposited at substrate temperature of 400 ^oC giving a sheet resistivity of 850 $\Omega/\square$. The optimum solution for SnO_2:F contains 28 wt.% $SnCl_4.5H_2O$, 39.5 wt.% C_3H_7OH, 29 wt.% H_2O, 1.5 wt.% NH_4F and 2 wt.% HCl giving a sheet resistivity of 75 $\Omega/\square$.

The highest conductivity of the film is obtained at 400^oC as shown in Fig.11. The variation of the sheet resistance with temperature is possibly due to the change in the films' stoichiometry and their structural properties. The resistivity of the films lowers as the doping is increased from 0 to 1.5%. This can be seen from Fig.12. Initially the undoped Tin Oxide films are filled with oxygen vacancies. These are filled by the Fluorine ions giving rise to an extra donor level. The resistivity will subsequently decrease. As doping by Fluorine is done beyond 1.5%, excess ions hinder the carrier mobility hence the resistivity rises.

Fig.13 shows transmission of the SnO_2:F film (graph a) to be 90% in the visible region and those of the SnO_2 films (graphs c & d) as having 81.5% in the same region. The transmittance of a lightly Fluorine doped film remains the same but there is a shift at the edge of the bandgap as seen in gragh (b). The conductivity of the former (doped film) is also higher. This means that doping produces higher transparency and conductivity. The transmittance of all the

34

films generally improves between wavelengths of 600 nm to 1100 nm. Beyond 2700nM, the transmittance of the film drops rapidly. This is mainly attributed to the poor transmittance of glass in the infra red region. Similar results as above have been reported by Abass et al.[26] and Amlouk et al [27].

The bandgap of the SnO_2:F films is obtained as 3.44 eV and for the SnO_2 films as 2.4 eV. Shewchun et al. has reported the bandgap of 3.42eV. SnO_2 is an n type material and according to Abass et al., its direct bandgap is 4.0 eV and the indirect bandgap is 2.6 eV.

The Power curve of an SnO_2/p-Si solar cell is shown in Fig.14. The cell parameters obtained are;

Open circuit voltage, V_{oc} = 110mA

Closed circuit current, I_{sc} = 45 μA

Fill Factor = 0.25

Cell efficiency = 0.002%

The efficiency of an SnO_2:F-p type silicon solar cell has also been reported to be low by other workers. These cells operate on the principle of minority carrier tunneling through an oxide layer. The silicon surface is accumulated by virtue of the SnO_2 workfunction. As a result the barrier height is increased hence few of the minority carriers (electrons) will tunnel through the Si-SiO_2 junction to combine with the photogenerated holes. This will greatly limit the photocurrent being drained from the cell.

3.7 CONCLUSION

SnO_2 and SnO_2:F thin films have been made using the spray pyrolysis setup. The former gave a sheet resistivity of 850 $\Omega/\square$ and the latter 75 $\Omega/\square$. The inhomogeinity of the films may be a possible cause for such a resistivity. The resistance between the film and the contacts may also add up to the existing resistance. Sheet resistivities in the range of 10-20 $\Omega/\square$ have been reported by other workers.

The transmittance of about 90% through the SnO_2:F films and their high conductivity are ideal for their application in transparent semiconducting photovoltaic devices.

The low efficiency can possibly be attributed to the incompatibility of the two materials, i.e small difference in work function between the tin oxide and p-silicon. This may however be improved by use of n-type Si. In addition, poor contacts, junction defects, high resistance of materials and surface reflections may degrade the efficiency of the cell substantially.

With this technique, it is possible to manufacture a large number of cells at very low cost.

SOLAR CELL FABRICATION BY VACUUM DEPOSITION

4.1 INTRODUCTION

The evaporation or sputtering of metals, alloys and compounds in a vacuum to condense as thin films on surfaces is a well established technique used for the manufacture, decoration and protection of a wide range of products. The earliest most important success of vacuum coating by evaporation was reported by Strong in 1933 when he deposited aluminium for front surface mirrors and later calcium fluoride for reducing the reflection of light from glass surfaces.

Thin films of the order of a few millionths of a centimeter, enough to obtain full optical properties of certain materials to a few thousandths of a millimeter for anticorrosion coating can be obtained. The process is free of chemical contamination, independent of electrical properties of the base material and the film finish is that of the base surface. The thickness of the film can also be monitored during deposition. Vacuum deposition has been used to coat glasses, plastics, ceramics, metals, paper and also substrates for solar cells.

4.2 EXPERIMENTAL SETUP

The vacuum coating system utilized is the Edwards E306A coating unit [28]. This system is capable of giving a vacuum of about 7×10^{-7} pa.
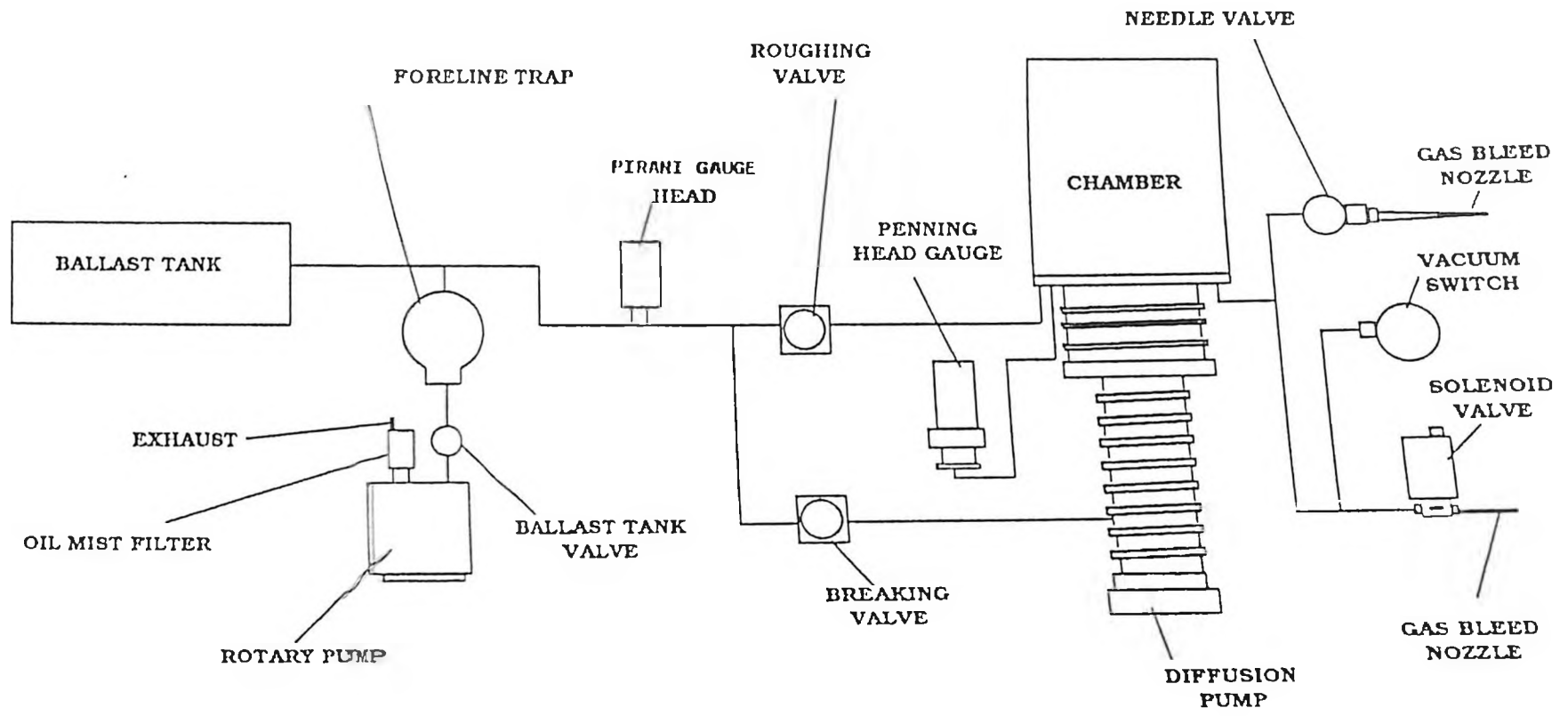
Fig. 15. Schematic Layout of the Edwards E306A Coating Unit

4.2.1 OPERATIONAL PROCEDURES

The layout of the pumping system is shown in Fig.15. The water supply is turned on followed by the rotary pump. This is allowed to run with the backing valve open. After the pressure has fallen to 30 Pa on the pirani gauge, the diffusion pump is switched on and allowed to run for twenty minutes to reach the working temperature. The backing valve is closed and the roughing valve opened. The high vacuum pump is then opened and the pressure allowed to fall. On reaching the desired pressure, evaporation of the chemical is done using low tension power. The sample can be retrieved from the chamber by admitting air.

To obtain desired properties of the semiconducting material during deposition, we designed a radiant heater to be incorporated into the vacuum chamber (Fig.16).
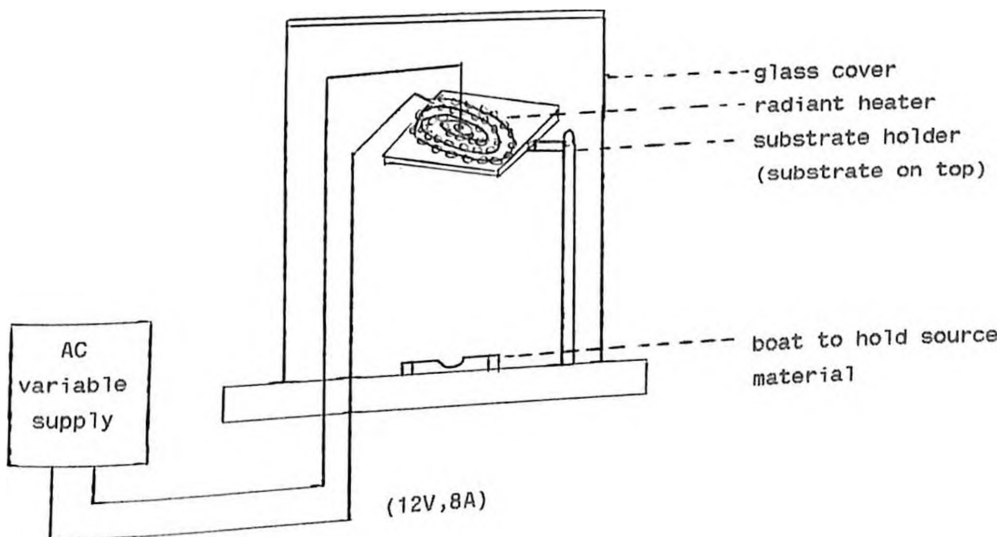
Fig. 16: Radiant heater incorporated in system.

The heater is made up of 70 cm Eureka wire passed through ceramic beads and then coiled making about five turns. The two ends are then connected to a variable ac power supply. The temperature in the chamber could reach about 150 ^{o}C in fifteen minutes.

4.2.2 SEMICONDUCTING MATERIALS

For this work, Indium Tin Oxide (ITO) is selected as a transparent semiconductor. The materials suitable as a transparent conductor must have a sufficiently large bandgap to ensure fundamental absorption edge to be below a wavelength of 0.3 μm, have a high infrared reflectivity and high transparency in the solar or visible region. Pure Indium Oxide has a direct bandgap of 3.75 eV.

4.2.3 SAMPLE PREPARATION FOR OPTICAL MEASUREMENTS

For optical measurements, standard glass slides (7.5x2.5 cm) are cleaned by a detergent and then by use of ultrasonic equipment. They are then exposed to alcohol vapour. ITO (initialy in form of solid pallet) is deposited on the slides using the coating unit to form a thin film. The glass slides are then placed in a furnace at various temperatures for about 90 minutes. The effect of annealing is studied on a spectrophotometer. The Perkin-Elmer Lambda 9 UV/VIS/NIR spectrophotometer is used to determine the transmittance of the film. The spectral range is setup, $0.3 < \lambda < 0.4$ μm uv region, $0.4 < \lambda < 0.8$ um visible region and $0.8 < \lambda < 3.2$ μm near infrared region. Back correction is done to set the ordinate display to 100% transmittance. The specimen is then run on the spectrophotometer for transmittance measurements.

4.2.4 CELL FABRICATION PROCEDURE

The substrate for the cell is 100 Ω-cm p type (111) boron doped silicon wafer. Silicon wafers are etched in hot Phosphoric acid for a few minutes. They are then cleaned with distilled water to remove surface ions and finally by acetone to get rid of grease particles. The wafers are dried in a furnace at 150 ^{O}C for a few minutes.

A mixture of HF and HNO_3 in the ratio 1:3 is a more versatile etching solution in place of the hot Phosphoric acid. The wafer is dipped in this solution (placed in a plastic container)for about 15 seconds and other cleaning procedure discussed above is used. However this mixture should be handled with caution as it is highly corrosive.

Aluminium is deposited on the back surface of the wafer. On the front surface ITO is deposited at a rate of 2 Å S^{-1}. The pressure in the chamber at which evaporation is commenced is 6 x 10^{-6} Pa. The substrate is heated by the radiant heater. Annealing the as deposited films in vacuum has been suggested by Campbell [29]. The sheet resistance of the film is reduced by such a process.

The sample is then placed in a furnace at 450 ^{O}C for one hour. After annealing the sample, a grid mask is placed on top of the ITO layer, and aluminium is deposited using the coating unit to form top contact .

4.2.5 ELECTRICAL MEASUREMENTS

The cell utilises optical energy to convert it into electrical. The current and the voltages generated by the cell are measured by

varying the resistance across the load (Fig.17).   The light I-V

characteristics are initially measured under direct sunlight at

about 80 mW/cm^2 insolation.   In the lab., a white light source is

used at an appropriate distance (25 cm) to give similar results.

The temperature of the cell is monitored by a copper-constantan

thermocouple.
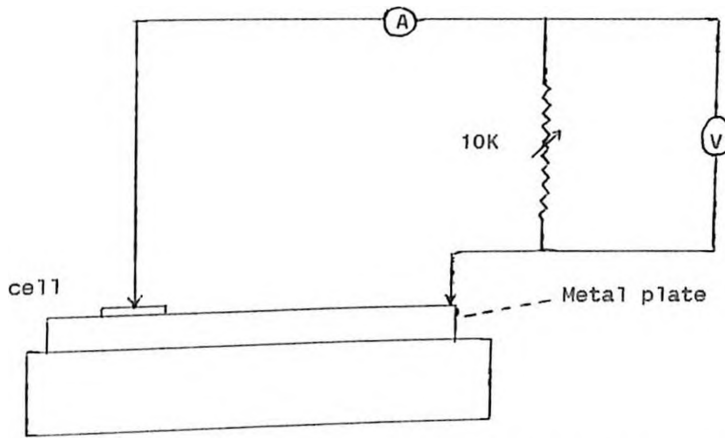
Fig. 17:   I-V Measuring setup of solar cell.

The dark characteristics of the cell are measured without the light

source (Fig.18).   The resistance across the cell is varied and the

current-voltage readings are recorded.
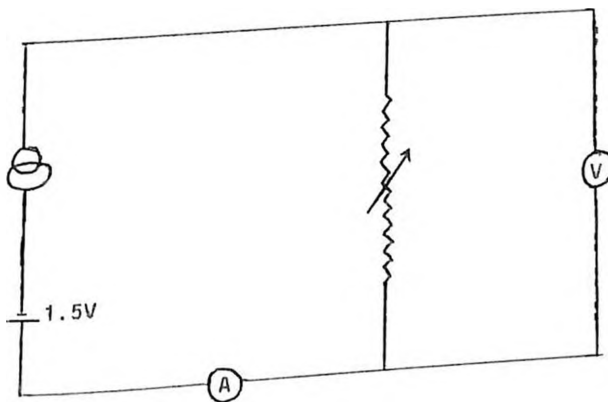
Fig. 18:   Dark I-V measurements.

42

The effect of temperature on the open circuit voltage and the short circuit current is investigated by varying the temperature of the cell. This is done by placing the test bench on a heater and monitoring the temperature by a thermocouple.

The minority carrier lifetimes through the cell was measured using circuit in Fig.19 [30]. A 555 clock pulse generator is used to provide a high frequency pulse. Pulse duration from a few milliseconds to about an hour can be obtained from this device.

Application of a negative going pulse to pin 2 triggers output pin 3 high. Pin 4 is connected to Vcc to be permanently high. To be used in the multivibrator mode, pin 6 is connected to pin 2 which triggers itself and runs freely. The frequency of oscillation is independent of the supply voltage.

The 74121 is a monostable multivibrator. It is triggered by either a slow DC level change from low to high (on pin 5) or by a gated negative pulse (pin 3 & 4). Pin 6 is used as an output and is connected to the 7408 AND gate. The diode is connected to the output of the AND gate. A 25 MHz oscilloscope is used to display the waveform.

43
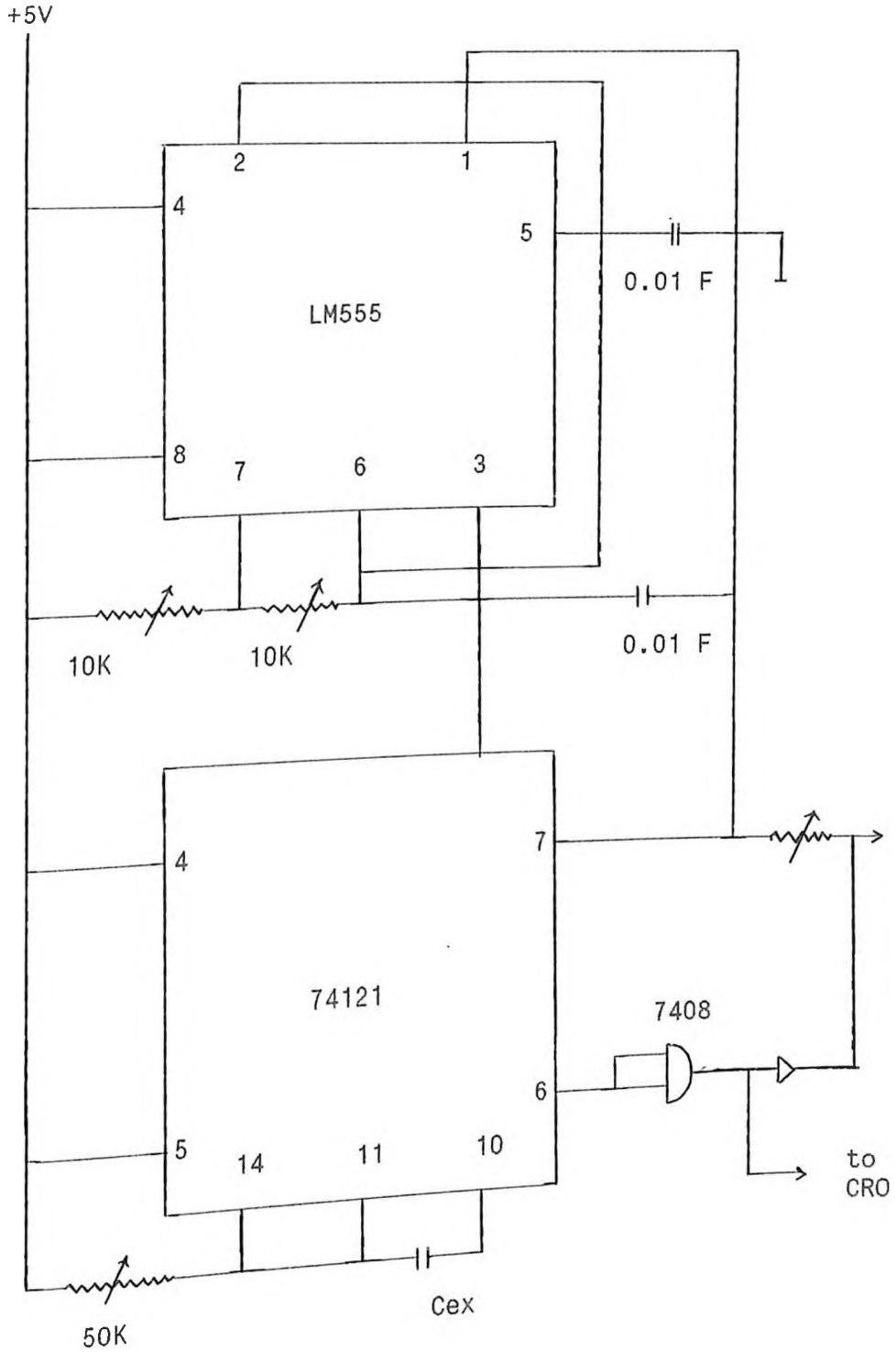
Fig.19: Circuit Diagram for Measuring Minority Carrier Lifetimes

44

4.3 RESULTS

Freshly deposited ITO films of about 1500 Å are dark brown in colour and almost opaque on visual inspection. The transmittance result from a spectrophotometer of an as grown ITO film is shown in Fig.20(a). This film is then annealed in air at 450 ^{O}C for 90 minutes and the resulting transmittance curve is plotted in Fig. 20(b).

ITO films are deposited on heated substrates. The transmittance of light through film fresh from vacuum chamber and one after annealing in air at 450 ^{O}C are shown in Fig.21(a) and 21(b) respectively.

The fabricated solar cell is illuminated at two different intensities and their power curves are drawn in Fig.22. Fig.23 shows the dark I-V characteristics of the cell.

The effect of temperature on the open circuit voltage and the short circuit current are shown in Fig.24 and Fig.25 respectively. Fig. 26 shows the waveform of a pulse through the cell. 10 - 50 μs pulses were used.
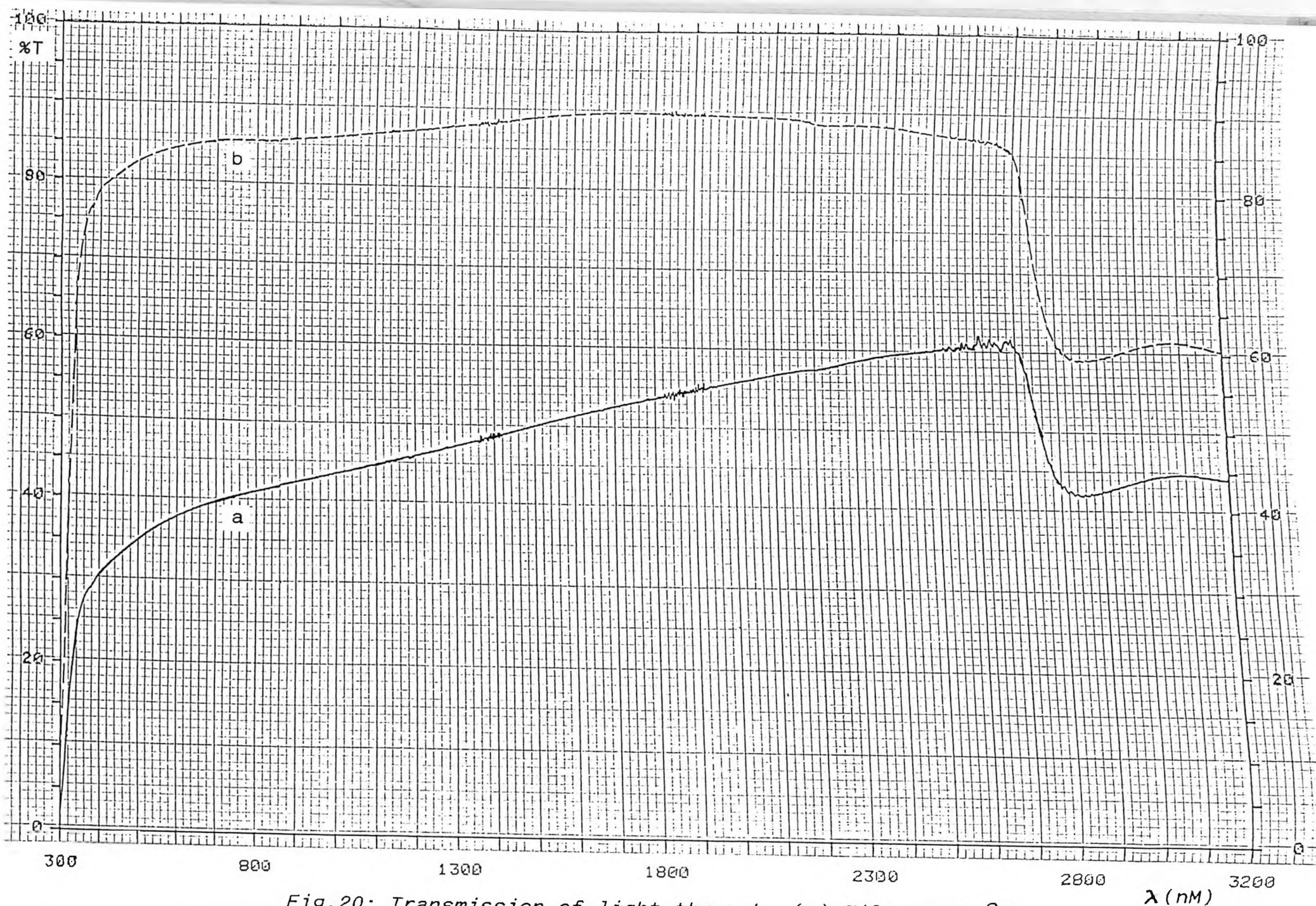
Fig.20: Transmission of light through, (a) Film at 25 °C,
(b) Film after annealing at 450 °C.

46
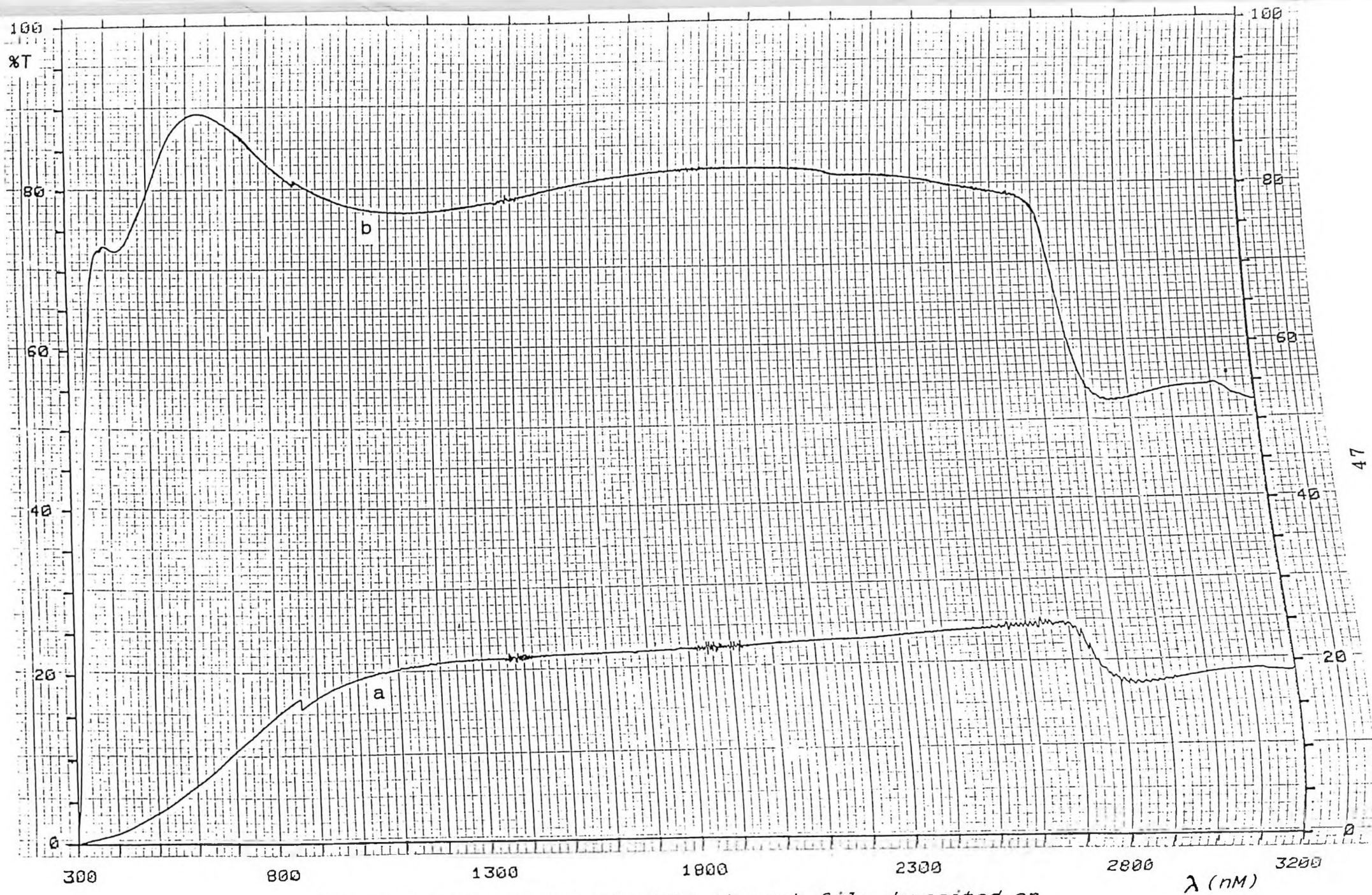
Fig.21: Transmission of light through film deposited on
heated substrate, (a) at 25 °C,
(b) after annealing in air at 450 °C.
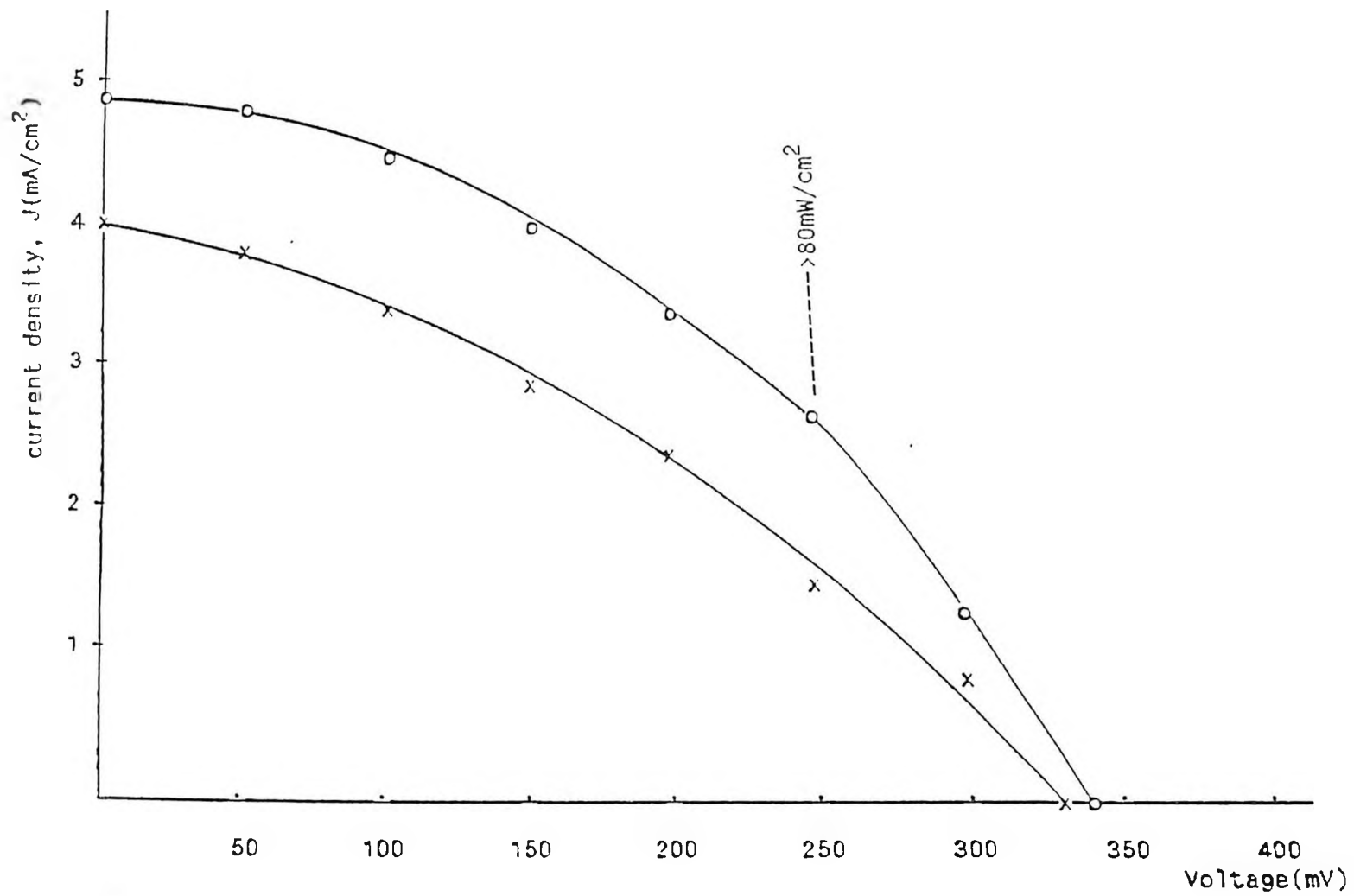
Fig.22: I-V power curves under two different illuminating intensities.

48
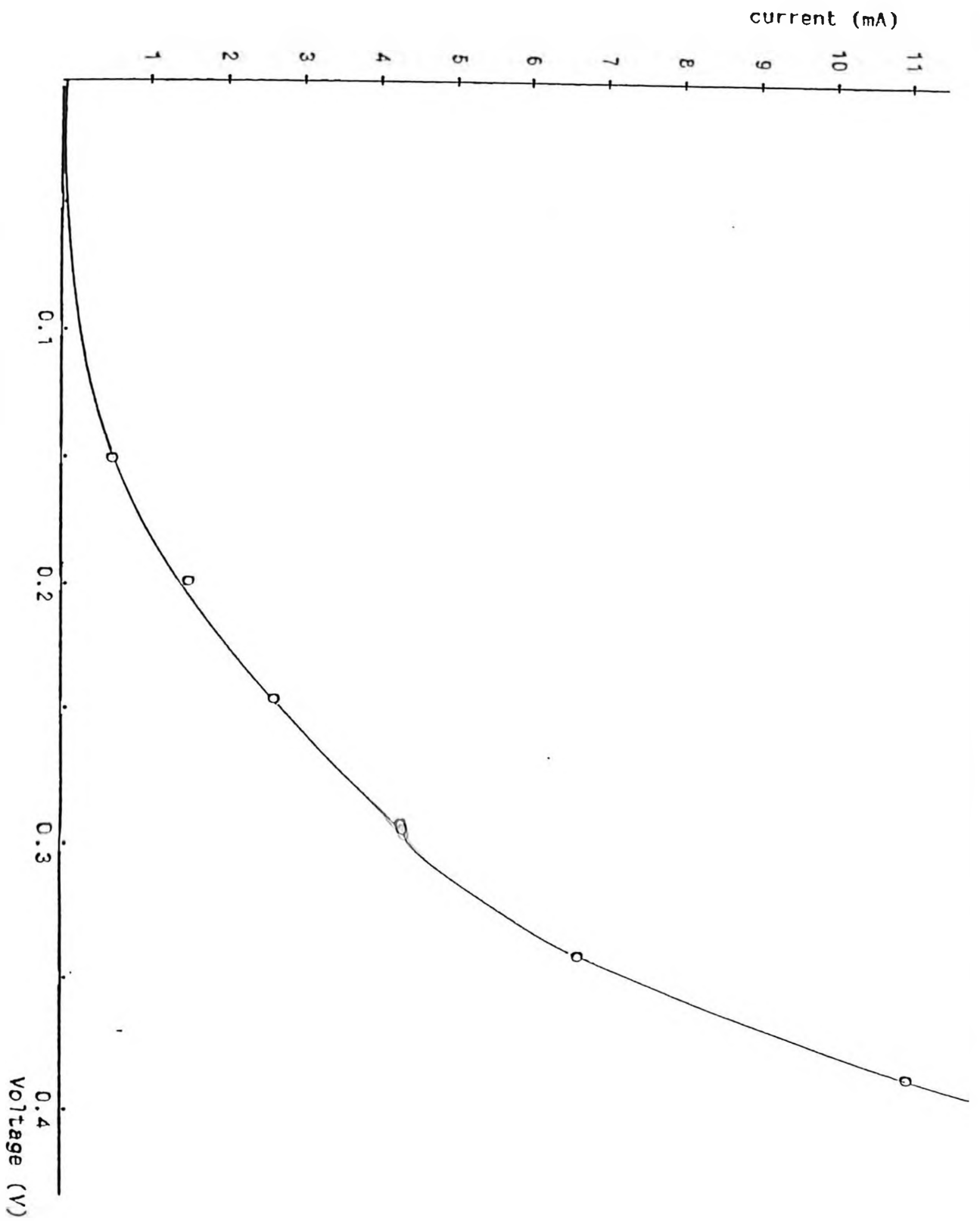
Fig.23: Dark I-V characteristics.

49
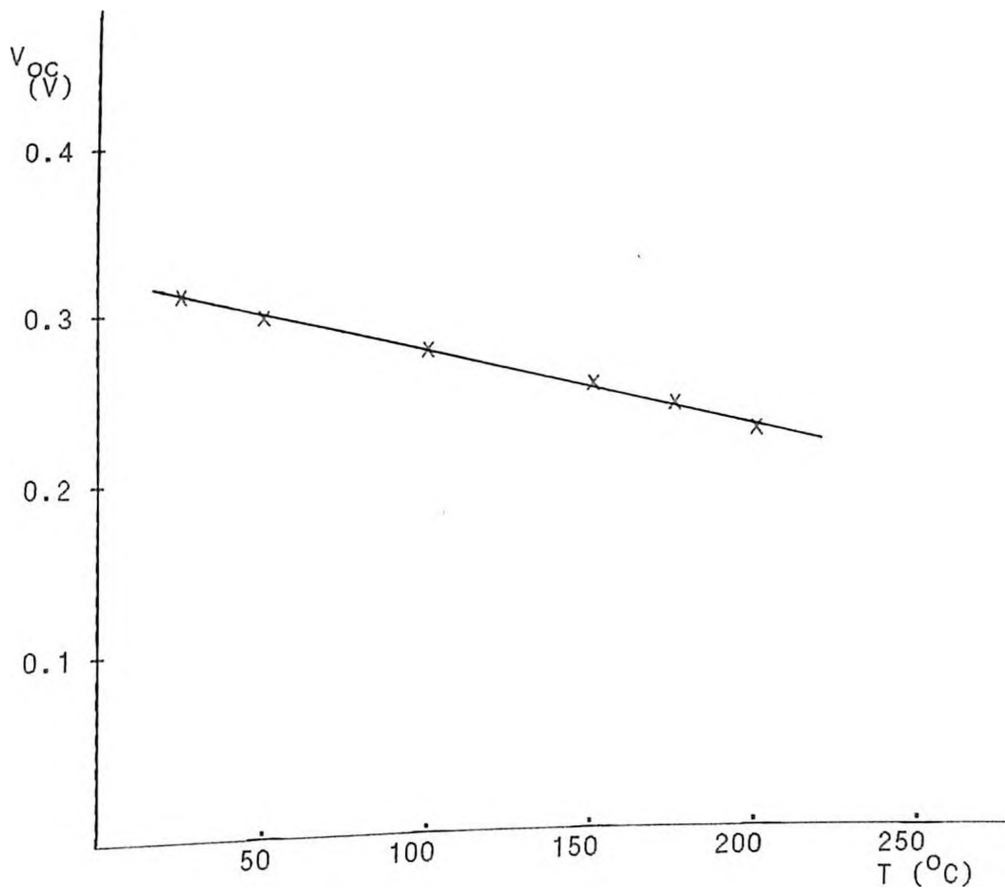
Fig.24: *Variation of open circuit voltage with temperature.*
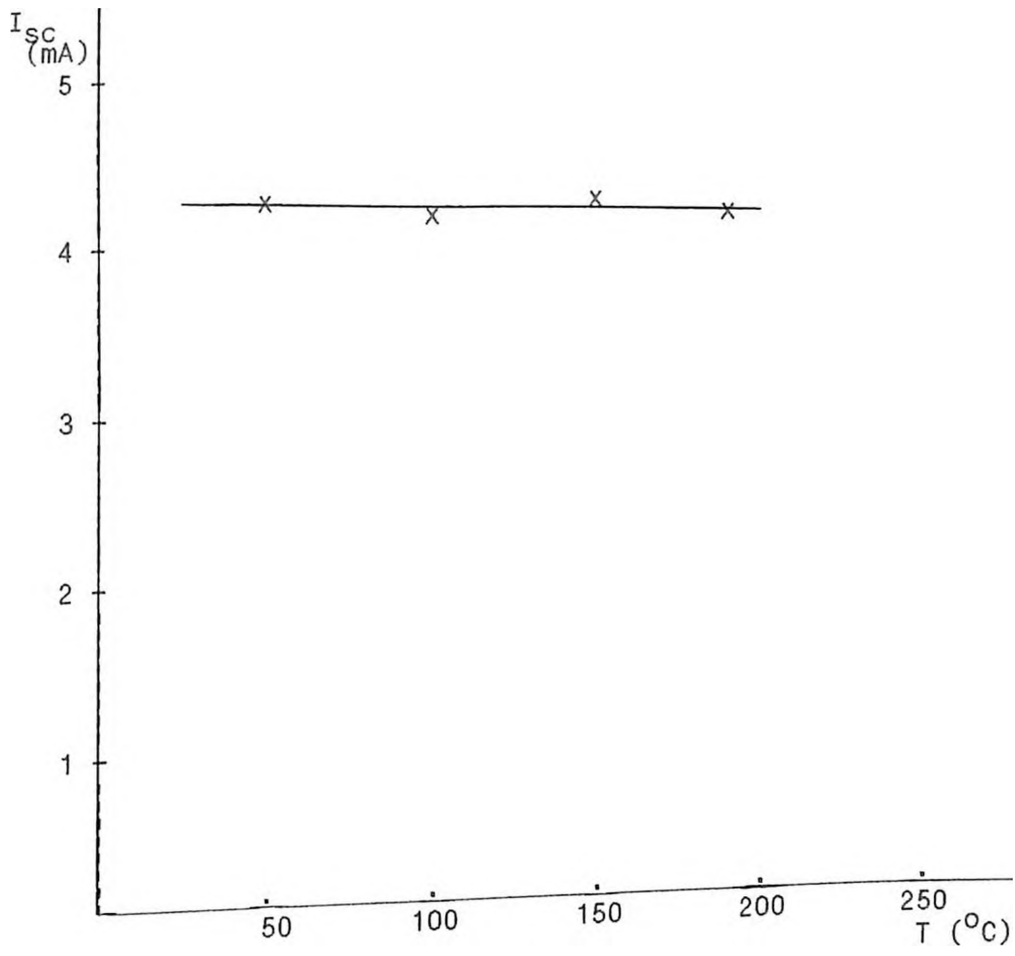
Fig.25: Variation of short circuit current with temperature.
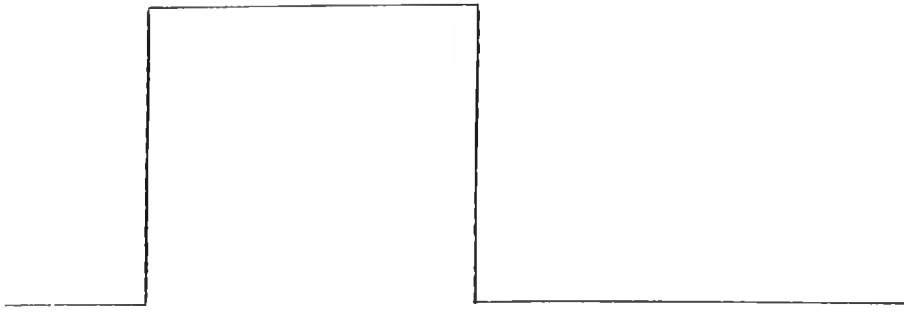
Input pulse
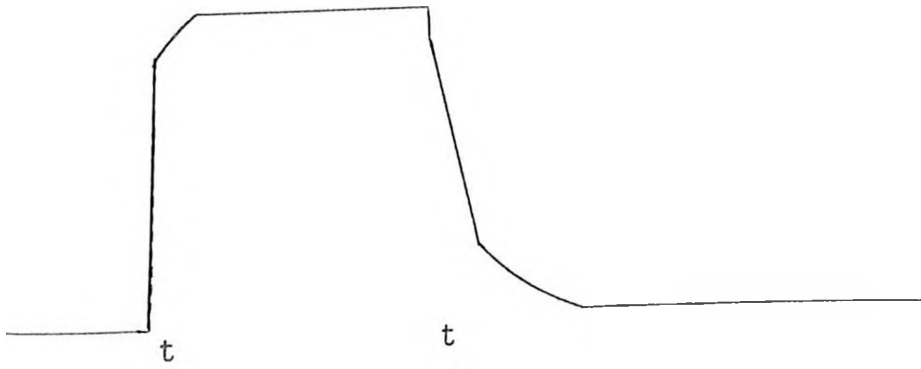
output pulse

Fig.26: Waveform of pulse through the cell.

4.4 DISCUSSION AND CONCLUSIONS

One of the criteria for the SIS cell operation is a transparent semiconducting window. ITO deposited at room temperature has a transmittance of less than 40% (Fig.20a) in the visible region of the spectrum. Majority of the photons are absorbed within the ITO layer and will not reach the bulk for any useful carrier transition to take place. The same ITO films annealed in air at 450 ^{O}C gives a transmittance of about 82% in the same region of the spectrum (Fig.20b). This result indicates that the transmittance has increased by twice the former case. This property may come up as a result of restructuring of the ITO lattices and extra Oxygen ions may be included in possible vacancies within this structure. ITO is known to exhibit both Hexagonal and body centered cubic (BCC) structures. The transmittance of the films increases with wavelength but falls off at the near infra-red region. This is mainly due to the glass surface[31].

Annealing temperatures above 450 ^{O}C did not give any marked improvement in the transmittance measurements. Films from vacuum chamber having been deposited on heated substrate gave a transmittance of about 10% in the visible region (Fig.21a). The same film on annealing at 450 ^{O}C gave a transmittance of 89% (Fig.21b). The rise in tramsmittance is very sharp between wavelenghths of 310 and 600nM. This indicates that the films have good optical characteristics. The conductivity of this films were also higher. ITO films deposited under this conditions are the best for solar cell fabrication. The above film thicknesses are of about

53

1500 Å but as the thickness is increased, the transmittance is expected to decrease slightly. Hamberg [32,33], has reported similar optical properties of ITO. It was not possible to increase the thickness of the ITO layer further as the tungsten boats on which evaporation was being done also vaporized contaminating the cell.

The cell was illuminated at two different intensities and the best light J-V characteristics of the cell from Fig.22 are:

V_{OC} = 340mV, J_{SC} = 4.9mA/cm^2, F.F = 0.404 and the efficiency n = 0.85%. The series resistance of the cell is about 13.3Ω.

With reduced illumination the cell parameters are:

V_{OC} = 330mV, J_{SC} = 4.0mA/cm^2, F.F = 0.363 and n = 0.6%.

From the latter results a decrease in fillfactor and efficiency is observed. Higher illumination is preferable for better device performance. From Fig.23 (with no illumination), the series resistance calculated is 14.3Ω. The cell has a very high series resistance and this may lower the efficiency of the cell. The resistance between the bulk material and the transparent semiconducting layer may be high. In addition to this, the contact between the top grid and the cell may be poor.

As the temperature of the cell is increased, the open circuit voltage decreases (Fig.24). This decrease can be as a result of changes in semiconductor transport properties viz. Fermi levels, lifetimes, bandgap, mobilities etc. The diffusion length in silicon increases with temperature rise since the diffusion constant remains

54

the same. Under normal operating conditions, the temperature may rise by about 20 ^{o}C. The test cell was however subjected to much higher temperatures mainly to investigate the effect at an extreme. The short circuit current is independent of the temperature as seen from Fig.25.

The carrier lifetime of the cell is about 9μS with changes in V_{oc}(mV) and t(μS) as 10 and 3.5 respectively (Fig.26). The higher the carrier lifetimes the better the efficiency. Most commercial cells have a carrier lifetime of about 30μS. Our cell has a low carrier lifetime in this respect and this may also contribute to the low efficiency.

With a thicker oxide layer, as may be the case in our cell, the light generated electrons from the ITO layer combine with holes in the SiO_2 layer giving rise to photosuppresion. In effect, the tunneling of the electrons is thus reduced resulting to lower current flow.

CHAPTER FIVE

CONCLUSION AND SUGGESTIONS FOR FUTURE WORK

5.1 CONCLUSION

Two techniques have been described and used in fabricating solar
cells.   They are relatively easy to use and inexpensive.
They can be summed up as shown in table 6;

Table 6: Some features of the deposition techniques.

SPRAY PYROLYSIS	VACUUM DEPOSITION
1. Easy to setup using locally available materials.	1. System not manufactured locally.
2. Can be used at relatively low temperatures.	2. Requires higher temperatures.
3. Approximately one hour time required before spraying.	3. Requires at least three hours of pumping.
4. Uniform film thickness may not be achieved.	4. Uniform film thickness can be achieved.
5. Film can be contaminated during deposition.	5. Film unlikely to be contaminated during deposition.
6. Sprayer just needs proper cleaning and can be reused as many times as possible.	6. Can be reused as many times as possible but spirals and boats have to be changed after being used for about three times.
7. Requires solution for deposition.	7. Uses mainly solids. For this reason, a wide range of materials can be used.
8. Cheap to maintain. Advisable to use in a fume chamber.	8. May be expensive to run and maintain. Water and electricity neccesary.

SIS silicon solar cells have been fabricated. SnO_2:F -p Si solar cells gave an efficiency of 0.002%. This efficiency is comparable for similar cells fabricated by other workers. It is however much lower than the 12% achieved for an SnO_2:F-n Si system reported by other workers [21]. The experimental setup of the spray pyrolysis system has been described.

ITO-p Si solar cells gave an efficiency of 0.85%. This is the highest value obtained for this type of cells in our laboratory so far. The properties of the materials have been studied and their importance in the SIS solar cells is outlined. For example, ITO has a wide bandgap (3.6eV), has a low workfunction (3.2eV), is highly transparent in the visible region of the spectrum, exhibits good conductivity and can be used as a partial AR coating with refractive index of about 2.

5.2 SUGGESTIONS FOR FUTURE WORK.

The first cell we fabricated did not exhibit any photovoltaic effect. On optimizing various parameters, a cell of 0.85% efficiency was achieved. During the course of this work, several observations have been made and would require further investigations. Keeping in mind that the ultimate aim is to obtain perfection, we can identify and consequently tackle each problem in its own merit thus keeping the experimental achievements as fruitful as possible.

A major problem encountered with the spray pyrolysis system is pollution. The user is prone to inhale and also be contaminated by

57

the hazardous fumes. The fume chamber reduces alot of the fumes but there is a need to reduce them to a minimum. A possible alternative is to spray in a well protected and ventilated chamber. The user may wear protective clothing and face masks.

The sheet resistivity of the SnO2:F film at 75 $\Omega/\square$ can be reduced further to as low as 10$\Omega/\square$. The spray solution can be modified further to achieve such a result. It should be worth fabricating SnO_2:F-n Si solar cells using this technique and obtain better efficiency. It is also possible to fabricate ITO-p Si solar cells using this technique with the spray solution being constituted by indium chloride, ethanol and distilled water mixed in appropriate ratios.

The silicon wafers used in this work has a resistance of 100 Ω-cm. Wafers with resistivities in the range 0.01 to 10 Ω-cm have been known to make more efficient cells. The thickness of the ITO layer should be increased to as high as 4000 Å. This layer is usualy degenerately doped and transparent. The carrier concentration will be increased and better anti-reflective properties can be acheived. We have been unable to achieve this as the boats cracked in the process. Increasing the evaporation leads within the vacuum chamber may solve this. Other methods like the electron beam source may also be tried.

The cleaning processes applied to the silicon wafers needs some improvements to reduce contamination, obtain better oxide growths and proper ohmic contacts. Contamination can results from dirty tools and improper handling of the wafers. The thickness of the

oxide layer needs to be optimized to about 20 Å. Some means of doing this is essential. Oxide thicknesses can be measured using ellipsometry. Aluminium and silver have been used to form the ohmic contacts. Whereas they are good conductors, some resistance still arises at the metal-semiconductor boundary. To improve the performance of the cell, this should be eliminated by reducing the grain-boundary effect and possibly form a free conduction zone.

It is important that at various deposition stages, the edges of the silicon wafer are well protected and masked to ensure that the device is not damaged or short circuited.

Other suitable semiconductors may be identified to be used in this configuration. Materials such as GaAs can be tried out in place of silicon.

Under the present working environment, i.e using un-sterilized equipment and laboratory, the targeted cell efficiency is about 1%. We are optimistic that the efficiencies of the cells can be greatly enhanced with improved fabricating procedures.

REFERENCES

(1) Encyclopeadia Britannica Vol 2, 769

(2) Fred Hoyle, 'Energy or Extinction', Heinemann Educational Books Ltd, (1977)

(3) Mcmullan J., 'Energy Resources and Supply', John Willey and Sons Ltd, (1976)

(4) Hunt, S.E., 'Fission, Fussion and the Energy Crisis', 2nd edition, Pergamon Press, 115 (1980)

(5) American Scientist, Sept/Oct (1976)

(6) Newsweek Magazine, 24, Sept 18 (1989)

(7) Newsweek Magazine, 8, May 12 (1986)

(8) Cheremisinoff, P. N., 'Principles and Applications of Solar Energy', Ann Arbor Science, (1978)

(9) Palz, W., 'Solar Electricity', Unesco, 179 (1978)

(10) Moore, T., 'Thin Films-Expanding the Market Place', IEEE Power Eng. Rev., Vol9 No11 p3-8 (1989)

(11) Charles, H. K., Ariotedjo, A. P., 'Review of Amorphous and Polycrystalline Thin Film Silicon Solar Cell Performance Parameters', Solar Energy, 329 Vol 24 (1980)

(12) Chu, T. L., Voltmer, F. W., 'Polycrstalline Silicon Solar
        Cells in Low Cost Foreign Substrates' , 229 Vol 17
        (1975)

(13) Willeke, G., Contactors Meeting (1st: 1886: Brussels,
        Belgium), 'Photovoltaic Power Generation', D. Reidel
        Publishing Company, (1987)

(14) Sze, S. M., 'Physics of Semiconductor Devices', John Willey &
        Sons, Chap. 14, 2nd Edition, (1981)

(15) Joshi, D. P.,'Theoretical study of the Photovoltaic Properties
        of Polycrystalline Si', J.Appl.Phy (59)8 (1986)

(16) S. Noor Mohammad, 'Theory of Saturation Photocurrent and
        Photovoltage in p-n Junction Solar Cells',
        J.Appl.Phy. 61(10) (1987)

(17) Ostoja, P., 'Characterization of Solar Cells', CNR, Bologna,
        Italy (1987).

(18) Shirley, Chu, T. L., 'Thin Film GaAs Homojunction Solar Cells
        on Recrystallized Germanium and Large Grain Ge
        Substrates', J.Appl.Phy. 60(2) (1986)

(19) Shewchun, J., 'Solar Energy Conversion', 843-864 (1978)

(20) Shewchun, J., Dubow, J., Myszkowski, A., and Singh, R., 'The
        Operation of the Semiconductor- Insulator-
        Semiconductor (SIS) Solar Cell', Journal of Applied
        Physics, 55, 49(2), Feb (1978)

(21) Vossen, J. L, Kern, W., 'Thin Film Processes', The Academic
Press, 257-321 (1978)

(22) 'Thin Film Symposium', Journal of Vacuum Science & Technology,
282 Vol.20 (1982)

(23) Eugene Coyle, 'Market for Photovoltaics', Fifth Int. Conference
on Alternative Energy Sources, Miami USA 1982,
461 (1983)

(24) Kaye, G. W., Tables of Physical and Chemical Constants,
Longman Group Ltd, 49 (1971)

(25) Singh, S. P. et al., 'SnO$_2$:F/n-Si and In$_2$O$_3$:Sn/n-Si SIS Solar
Cells', Thin Solid Films, 127, 77-84 (1985)

(26) Abass, A. K., 'Optical Properties of Fluorine Doped SnO$_2$
Films', Journal of Applied Phys., 59(5) March (1986)

(27) Amlouk, M., et al, 'Structural, Optical & Electrical Properties
of SnO$_2$:F and CdS Airless Sprayed Layers',
Solar Energy Materials, Vol.15 No.6 (1987)

(28) 'Edwards E306A Vacuum Coating Manual', BOC Limited,
England (1982)

(29) Campbell, D. S., Saim, H. B., 'Properties of Indium-Tin-Oxide
(ITO)/Silicon Heterojunction Solar Cells by Thick
Film Techniques', Vol.15 No.4, Solar Energy Materials
(1987)

(30) Benson A. Ogola, 'Fabrication and Characterization of Silicon Solar Cells', M.Sc. Thesis, University of Nairobi, (1985)

(31) Sreenivas, K., et al, 'Preparation & Characterization of rf Sputtered Indium Tin Oxide Films', J.Appl.Phy. 57(2) (1985)

(32) Hamberg, I., 'Indium- Tin- Oxide Films: Basic Optical Properties and Applications to Energy Efficient Windows', Ph.D Thesis, Chalmers University of Technology, Sweden (1987)

(33) Hamberg, I., Granqvist, C., 'Evaporated Sn Doped In_2O_3 Films, Basic Optical and Applications to Energy Efficient Windows.', J.Appl.Phy. 60(11) (1986)

Pascal program to calculate quantities of stannic chloride, propanol and water in solution.

```pascal
Program chemi (input,output);
 Var a,b,c:real;
 procedure calculate (a,b,c:real);
  const density= 0.785;
        weight= 100.0;
  var q,vol1,vol2:real;
      modifier,newweight:real;
   begin
    if (a+b+c)<=100.0 then
     begin
      writeln('input total weight required (g)');
       writeln;
        readln(newweight);
         writeln;
          modifier:=newwweight/weight;
         q:=a*modifier;
        vol1:=(b/density)*modifier;
       vol2:=c*modifier;
      writeln('mass of tinchloride(g):',q:6:3, 'Vol. of propanol:'
               :19,vol1:5:3, 'Vol. of water:':16,vol2:5:3)
     end
    else
     writeln('ERROR re-enter % values')
    end;
  begin
   writeln('Input % values of tinchloride, Propanol & Water');
    readln(a,b,c);
end.
```

current and voltage values under
dark conditions (Fig.23)

V (V)	I (mA)
0.05	0.20
0.10	0.35
0.15	0.60
0.20	1.55
0.23	2.10
0.25	2.65
0.27	3.00
0.30	4.20
0.35	6.65
0.37	8.20
0.40	11.00

variation of sheet resistance with temperature (Fig.11)

Temp. (^oC)	R ($\Omega/\square$)
330	81.0
350	77.5
370	76.0
390	75.5
400	75.0
410	75.7
430	78.5
450	81.5
470	87.0

APPENDIX A4

sheet resistivity at variuos F concentration (Fig.12)

% F	R ($\Omega/\square$)
0.0	850
0.5	360
1.0	165
1.25	125
1.5	75
2.0	205

APPENDIX A5

variation of current density with voltage
of an SnO_2:F-p Si solar cell (Fig.14)

V (mV)	J ($\mu A/cm$)
0	45
10	41
20	36
30	33
40	30
50	24
60	20
70	16
80	12
100	4
110	0

APPENDIX B1

current density and voltage values of ITO cell
at two illuminating intensities (Fig.22)

V (mV)	J (mA/cm²) at 80mW/cm²	J (mA/cm²) < 80mW/cm²
0	4.90	4.00
24	4.84	3.90
50	4.75	3.85
74	4.65	3.65
100	4.55	3.40
126	4.30	3.25
150	4.05	2.90
175	3.60	2.25
200	3.40	2.45
226	2.95	1.90
250	2.70	1.40
300	1.35	0.80
330	-	0.00
340	0.00	-

open circuit voltages at different
temperatures. (Fig.24)

T (°C)	Voc (V)
25	0.310
40	0.306
50	0.300
60	0.296
75	0.292
90	0.285
100	0.280
110	0.276
120	0.272
150	0.260
175	0.255
200	0.238

APPENDIX B4

short circuit current at various
temperatures. (Fig.25)

T (^{o}C)	Isc (mA)
25	4.20
35	4.20
50	4.30
75	4.20
90	4.25
100	4.20
110	4.20
120	4.15
140	4.20
150	4.25
170	4.20
190	4.20